Republic of Iraq
Ministry of Higher Education
and Scientific Research
University of Babylon
College of Education for Pure Sciences
Department of Physics

Effect of Silicon Carbide on the Electronic and Spectral Properties of the PVA/SeO_2 Structure. A Density Functional Theory Study

A Thesis
Submitted to the Council of the College of Education for Pure Sciences, University of Babylon in Partial Fulfillment of the Requirements for the Degree of Master in Education / Physics

By

Safa Zuhair Hussein Abbas

B. E. Sc. (Physics)
(University of Babylon 2010)

Supervised by

Assist. Prof. Dr. Hind Ahmed Mohammed Roof Yasin

2022A.D. **1444 A.H.**

بِسْمِ ٱللَّهِ ٱلرَّحْمَٰنِ ٱلرَّحِيمِ

« وَمَا يَعْزُبُ عَن رَّبِّكَ مِن مِّثْقَالِ ذَرَّةٍ
فِي الْأَرْضِ وَلَا فِي السَّمَاءِ وَلَا أَصْغَرَ
مِن ذَٰلِكَ وَلَا أَكْبَرَ إِلَّا فِي كِتَابٍ مُّبِينٍ »

صَدَقَ اللهُ العَلِيُّ العَظِيمُ

سورة يونس الآية ٦١

Dedications

To My country with honor and dignity...

To an absent never forgotten but remembered everywhere, my late father and grandmother...

To the source of strength and tenderness, my mother...

To my wonderful sweet sister, Saba...

To my brothers and my beloved family; Sadik, Ali Z., Ali W., Noor al Huda, Maryam, Layn, Lamar, Tallin...

To my supervisor, Dr. Hind Ahmed...

To my co-workers who helped me; Dr. Jaber Al-Hamdani, Mr. Mohammed Salem, Mr.Ayad, Mrs. Hawraa, Mrs. Shaima, Mr. Hussein Ali, Mr. Mohammed S., Mr. Thamer.

To my teachers who taught me Mr. Yousif H. Abdul Hussain and Mr.Mohammed Abd-ALKadhim.

To my close friends and colleagues who have supported me all the way; Zainab, Rashaq, Shaima, Ahmed, Muhannad, Fatima...

I dedicate this work.

SAFA...

Acknowledgments

Thankfulness, praise be to Allah, the grace that befits his holy self, and peace and blessings be upon our Messenger, Muhammad Bin Abd Allah, May Allah's prayers and peace be upon him and his family and companions.

I would like to express my deep gratitude and appreciation to my supervisor, Dr. Hind Ahmed who contributed with his abundance knowledge, his valuable time and his sincere help in helping me to traduce this research,

Thanks to the Deanery of the College of Education for the Pure Sciences / University of Babylon and the Department of Physics for offering me the opportunity to complete my research. I also would like to express my thanks to all teachers, instructors and students of the Department of Physics for their assistance especially Dr. Khalid Haneen, Dr. Shurooq Sabah.

I would like to express my deep appreciation to all members of my family for their material and spiritual support.

Finally, thanks to all my friends and all those who have supported me in doing this research. I wish success to all.

SAFA...

Summary

The effect of increasing the number of atoms on the geometrical, electronic and spectral properties of the nanocomposites (PVA-SeO_2-SiC) (Polyvinyl alcohol - selenium dioxide - silicon carbide) was studied using Gaussian 0.9 with the help of Gaussian View 0.5.

All calculations were carried out using the Density Functional Theory (DFT), and the exchange - correlation interaction is described by the Becks 3-parameter Lee - Yang - Parr (B3LYP) hybrid functional with in the General Gradient Approximation (GGA) with (LanL2DZ) basis sets.

The geometrical, electronic and spectral properties of the polymer (polyvinyl alcohol) (PVA) (43Atoms) were studied, and then the effect of adding silicon carbide (SiC) nanoparticles to the polymer (PVA) was studied to become the (PVA-SiC) (45Atoms) nanocomposite and then adding of (SeO_2) nanoparticles in two-stage (PVA-SeO_2-SiC) (46Atoms) and (PVA-SeO_2-SiC) (90Atoms).

The geometrical properties included improving geometric optimization (bonds and angles). The electronic properties included (Ionization potential, Electron affinity, Chemical hardness, Chemical softness, Electronegativity, Total energy, cohesive energy, energy gap, Electrophilicity and density of states) as well as spectral properties, which included (IR, Raman, UV-Visible, and NMR). The results showed that increasing the number of atoms of the nanocomposites had a direct effect on all the properties of the studied structure.

The addition of nanoparticles and increasing the number of their atoms successively led to a significant improvement in the studied properties, including the energy gap, which decreased from (6.856eV) for the (PVA) polymer to (1.848eV) for the (PVA-SeO_2-SiC) (90Atoms) nanocomposite. A significant improvement was also observed in the electronic properties, as the results showed the binding energy, ionization potential, electronegativity, electronic affinity, chemical softness, and polarization of the composite (PVA-SeO_2-SiC) increased, while the chemical hardness decreased. It found that there are different shapes of electrostatic potential and density of states in each structure. In general, the results of this study refer to the construction of new structures that have different new electronic properties.

Contents

List of Symbols and Abbreviations	
Symbol	***Physical Meanings***
B3LYP	Becke’s, Lee, Yang, and Parr's
η	Chemical Hardness
K	Chemical Potential
S	Chemical Softness
E_{coh}	Cohesive energy
CGF	Contracted Gaussian function
DFT	Density Functional Theory
DOS	Density of States
$\hat{f}_i$	Eigenfunction of the operator
EA	Electron Affinity
$\rho(r)$	Electron Density
X	Electronegativity
ω	Electrophilicity
ESP	Electrostatic Potential
E	Energy
E_g	Energy Gap

E_{HOMO}	Energy of the Highest Occupied Molecular Orbital
E_{LUMO}	Energy of the Lowest Unoccupied Molecular Orbital
V_{ext}	External Potential
FTIR	Fourier Transform Infrared Radiation
ν	Frequency
GIAO	Gauge-Included Atomic Orbital
GV5	Gauss view 5.0.8
G09	Gaussian 09
GTO	Gaussian Type Orbital
GGA	General Gradient Approximation
HF	Hartree-Fock
HOMO	Highest Occupied Molecular Orbital
HK	Hohenberg-Kohn
F_{HK}	Hohenberg-Kohn Operator
IR	Infrared Ray
IP	Ionization potential
T	kinetic energy
$\hat{T}$	Kinetic energy operator

C	Light Speed in Vacuum
$\hat{P}$	Linear momentum operator
LDA	Local Density Approximation
LSDA	Local Spin Density Approximation
LUMO	Lowest Unoccupied Molecular Orbital
MO	Molecular orbital
NMR	Nuclear Magnetic Resonance
ppm	Parts per million
h	Plank constant
PVA	Polyvinyl Alcohol
$\hat{V}$	Potential energy operator
SeO_2	Selenium Dioxide
SiC	Silicon Carbide
STO	Slater Type Orbital
$\hat{V}_{ne}$	The Attractive Interactions between Nuclei and Electrons Operator
J	The classical Coulomb energy
ε_i	The corresponding energy
$\hat{T}_e$	The Electronic Kinetic Energy Operator

$\widehat{H}$	The Hamiltonian Operator
∇^2	The laplacian Operator
E_{NC}	The non-classical electron–electron interaction energy
N	The Number of Electrons
$\hbar$	The Reduced Planck Constant
$\widehat{V}_{ee}$	The Repulsive Electron– Electron Interactions Operator
P	Total Dipole Moment
E_{tot}	Total Energy
UV	Ultra-Violet
UV-Vis	Ultraviolet-Visible
VDZ	valence double-zeta
VTZ	valence triple-zeta
Ψ	Wave function
ψ_i	Wave Function Molecular Orbitals
λ	Wavelength of Photon

List of Figures

List of Tables

Chapter One

Introduction and Literature Review

1.1 Introduction

Nanoscience is one of the most important research and development activities in the border of modern science. The use of nanoparticle materials provides many unique advantages. Due to the large volume-surface ratio, Nano-sized materials show different physical and chemical properties in comparison to bulk materials [1].

In recent years, materials with suitable and sustainable properties have drawn worldwide community attention. The purpose of doping a variety of materials to enhance of their properties. The factors the most influencing of these properties depend on the nature and the method of their synthesis. The developing desired devices required determining the cost, guide researchers, and knowing the field of applications, then selecting the materials and technology. Nanocomposites and polymer blends are attracting increasing attention from scientists and researchers due to their use in many industrial sectors [2].

1.2 Polymers

For the first half of the twentieth century, it was generally understood that polymers did not conduct electricity. While inorganic solids were known to possess a wide range of different electrical properties, including conductivity, semi-conductivity and insulation, polymers were very much confined to being insulators [3].

Although many people probably do not realize it, everyone is familiar with polymers. They are all around us in everyday use, in rubber, in plastics, in resins and in adhesives and adhesive tapes, and their common structural feature is the presence of long covalently bonded chains of atoms. They are an extraordinarily versatile class of materials, with properties of a given type often having enormously different

values for different polymers and even sometimes for the same polymer in different physical states [4].

Polymers are one of the most widely used materials, due to their versatile properties. Polymers contain properties that make them unique and virtually irreplaceable. In general, polymers are known for their low density with intermediate stiffness and strength. Although polymers have ideal properties for a wide range of applications, they were unable to be used for applications requiring electrical conductivity. When there was the addition of a conductive filler particle, it was discovered that a polymer would allow the flow of current through its system. This increased the number of industrial applications for polymers [5].

Polymer molecules are made up of a series of repeating units, known as monomers, that are joined together by covalent bonds to form larger molecules. A polymer can have any number of units, denoted by the letter n, which is referred to as the degree of polymerization. The simplest polymer is composed of n monomers linked together by covalent bonds to create a linear chain. Additionally, polymers can have branching geometries, in which a single monomer functions as a node that connects many monomers. Controlling branching experimentally has resulted in the creation of polymer configurations like as stars, combs, rings, and brushes [6].

1.3 Composite

A composite is a material made with several different constituents intimately bonded this definition is very large. A more restrictive definition is used by industries and scientists: a composite is a material that consists of constituents produced via a physical combination of pre-existing ingredient materials to obtain a new material with unique properties when compared with the monolithic material

properties. The components cannot be separated by the naked eye and function together fundamentally [7].

The composites have been widely used in various fields such as military equipments, safety, protective garments, automotive, aerospace, electronics and optical devices. However, these application areas continuously demand additional properties and functions such as high mechanical properties, flame retardation, chemical resistance, UV resistance, electrical conductivity, environmental stability, water repellency, magnetic field resistance, radar absorption, etc. [8]. The optical properties of polymers constitute important aspects in the study of electronic transition and the possibility of their application as optical filters, a cover in the solar collection, selection surfaces and green house. The information about the electronic structure of crystalline and amorphous semiconductors has been mostly accumulated from the studies of optical properties in a wide frequency range [9].

1.4 Polymer Composite

Polymer composites are becoming important for multiple technical applications in various fields [10]. Since the composite polymers consist of the addition of different materials to increase the homogeneity of the polymers in the matrix to change some of its characteristics and create new characteristics [11]. The unique properties of such composites make them technologically superior and more cost-effective than alternative material. Conducting polymer composites have been adapted for a variety of applications. The basic applications for conductive vehicles include protection from electromagnetic interference [10].

1.5 Nanocomposite

"Nano" is a small word but the technology associated with it has changed the world in an incredible way. Now a day's nanotechnology has affected and is changing the existing technology in a farfetched way. The characteristics of overlapping nanocomposites have to be studied because of their scientific, industrial, electrical, and medical importance. As a result, it attracted interest and directed scientists and researchers to investigate its structure, electrical properties, and other properties.

The Nanocomposite is a compound substance of two or more substances, one of which is the base and the other is additive provided that the added substance is in nanometer dimensions. Since the additive is within the nanoscale, significant changes will occur in the properties [12]. The nanocomposite may use added fibers such as carbon fibers or glass fibers or may use nanoscale materials such as gold, silver, diamond, copper and silica Carbon nanotubes give the nanocomposite strength and stiffness high at low concentrations [13].

1.6 Polymer Nanocomposite

Polymer nanocomposites have gained important research and industrial interests due to their excellent possibility for variable applications. The field of nanotechnology has been a very exciting topic and it can make our lives better and make all the world the best venue to live in. Polymeric nanocomposites consist of a copolymer or polymer having nanoparticles or Nano fillers scattered in the polymers matrices [14]. The installation of the polymer nanocomposites is an integral aspect of nanotechnology of the polymers. By inserting the nanometric inorganic

compounds, polymer nanocomposites represent a modern alternative to traditionally filled polymers [15].

Polymer nanocomposites are mixes of polymers and inorganic components with at least one nanoscale dimension. By controlling the microscopic morphology of bulk polymer nanocomposite properties, it is possible to significantly improve their optical, dielectric, mechanical, and thermal characteristics. This enables the tuning of polymer nanocomposites to suit a variety of applications, including fire-resistant textiles, fuel cells, solar cells, and even aircraft surfaces [16]. Nanoparticles with various compositions are prepared by physical and chemical methods. The physical methods include evaporation, sputtering, laser ablation, ion ejection, and electron-beam lithography [17].

1.7 The Raw Materials

1.7.1 Polyvinyl alcohol (PVA)

Polyvinyl alcohol (PVA) is in the form of white granules [18]. PVA has attractive properties such as the ability to dissolve in water and its resistance to the action of solvents and oils and has an exceptional ability to adhere to cellulosic materials, so it has wide uses. High tensile strength and storage capacity, and electrical and optical properties depending on the type of impurities added [19]. It is a non-toxic, biocompatible synthetic polymer, that has good transparency and high dielectric strength [20]. PVA is a cheap polymer and is eco-friendly having excellent film forming and adhesive properties, good chemical and mechanical stability and high potential for chemical cross-linking [21]. It has a carbon chain backbone with hydroxyl groups attached to methane carbons/these (OH) groups can be a source of hydrogen bonding and hence assist the formation of polymer composite, polyvinyl

alcohol semi- amorphous [22]. The degree of polymerization of PVA (of formula $[CH_2CH(OH)]_n$ with « n » is the number of monomers in a macromolecule) is related to the degree of hydrolysis (each monomer contains one OH groupment) and both affect its solubility. It is well known that when the degree of polymerization of PVA increases, its molecular weight increases. It has been shown that, at a given temperature, the solubility of PVA decreases with increasing molecular weight [23,24,25].

Table (1.1): Physical and Chemical Properties of Polyvinyl Alcohol (PVA) [26]

Property	Description
Appearance	White to an ivory white granular powder
Molecular formula	$(C_2H_4O)_n$
Solution PH	5- 6.5
Density (g/cm^3)	1.3
Refractive index	1.55
Glass transition temperature T_g (^oC)	85
Melting temperature T_m (^oC)	230

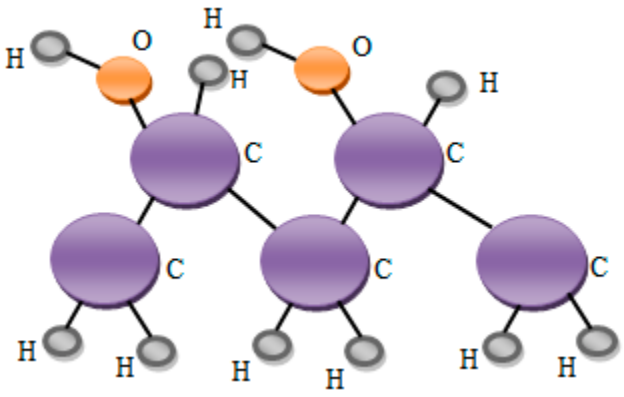

Fig. (1.1): The structure of Polyvinyl alcohol (PVA) [27]

1.7.2 Silicon Carbide (SiC)

The (SiC) nanoparticles have good electrical, thermal, optical, chemical and mechanical properties, so it has been used for different electronic and optoelectronic applications [28].

Silicon carbide (SiC) is a highly covalent material, including 88% covalent bonds and 12% ionic bonds, which makes it own excellent overall properties including high modulus, high stiffness, high melting point, and corrosion resistances [29]. It is a promising filler material due to its good thermal and chemical stability [30]. SiC is highly wear resistant and has also good mechanical properties. Table (1.2) shows some physical and mechanical properties of SiC [31].

Table (1.2): The Physical and Mechanical Properties of Silicon Carbide (SiC) Nanoparticles [31]

Property	Description
Density (g/cm^3)	3.21
Melting point (^oC)	2730
Colour	Black
Boiling point (^oC)	4100
Thermal conductivity (w/m.^{o}c)	84
Young modulus (GPa)	430

1.7.3 Selenium Dioxide (SeO_2)

Selenium is a common volatile element in coal and mineral [32]. In 1990, selenium was listed as one of the hazardous air pollutants in the Clean Air Act Amendments (US) [33].

In 2011, the emission of selenium in coal-fired plants was firstly regulated by US Environmental Protection Agency (EPA) [34]. With the strict standard for coal-fired plants in the future, more attention has been attracted to selenium control technologies.

Under high-temperature oxidizing atmosphere, SeO_2 is released as the main product of selenium compounds in coal-fired flue gas [35]. As a low-cost sorbent for SO_2 [36].

Selenium in coal converts to toxic SeO_2 during the combustion process, and SeO_2 can easily migrate to water to form a more toxic selenite [37]. It is widely known that selenium with low concentration is one of the essential nutrients for humans. However, if overdosed, it may cause digestive dysfunction, hair and nail damage, and neurological damage to the humans body [38,39].

1.8 Literature Review

B. K. Agrawal, *et al.* in (2012) [40] investigated Density Functional Theory study of small SiC nanoclusters, by using DFT - B3LYP method. Studied the optimized structures of SiC, electronic properties (HOMO–LUMO Gap, ionization potential and electron affinity) and Vibrational Properties (IR and Raman). The results of the study showed that the structures containing the maximum number of carbon atoms are most stable whereas the clusters containing the maximum number of silicon atoms have low binding energies. Also, the absorption spectra for all the clusters appear in the far ultra-violet region. The absorption shows strong peaks at different energy locations that characterize the nanoclusters. Quite weak absorption is seen in the visible region.

R.S. Singh in (2016) [41] revealed to Hydrogen adsorption on sulphur-doped SiC nanotubes, the adsorption properties are investigated by electronic band structures, density of states (DOS), adsorption energy and population analysis calculations for intrinsic SiCNT adsoprtion and adsorption on S-doped C-sites and Si-sites of SiCNT, by using density functional theory. The results of the study showed that band gap is decreasing and there is no significant effect on electronic structure.

A. Hosseinian, *et al.* in (2017) [42] employed DFT with B3LYP/6-31G(d) method to study optimization of structures, energy calculations, and density of states (DOS) analysis of graphene, SiC, BN, and AlN nanosheets as anodes in Na-ion batteries. The results of the study showed that the HOMO and LUMO energies of

the SiC nanosheet are reduced about −3.68 and −3.47 eV, respectively and the E_g is reduced from 0.21 to 0.18 eV.

M. Peyravi, *et al.* in (2019) [43] studied a chemisorption of selenium dioxide on $C_{19}X$ (X=Ni, Cr and Cu) nanocage by DFT-based calculation, using the first-principles density functional theory (DFT) method. Was studied molecular electrostatic potential, binding energy, geometric parameters, transferred charges, frontier molecular orbitals, dipole moments and the global indices. The results of the study showed that the $C_{19}Cr$ shows an extraordinary binding energy toward the SeO_2(II) by significant changes in electronic properties. Additionally, the $C_{19}Cr$ nanocage is a unique adsorbent to the adsorption of SeO_2.

A. Hashim, *et al.* in (2019) [44] investigated the effect of increase the number of SiC nanoparticles atoms on the optimized geometrical parameters, electronic and spectroscopic properties of polyvinyl alcohol, by using the Gaussian 0.9 program with help of Gaussian View 0.5 using density functional theory (DFT) with local spin density approximation B3LYP level and6-31Gbasis sets. Was studied structures are (PVA)(43Atom), (PVA-SiC)(35 Atom) and (PVA-SiC)(51Atom) nanocomposites. The results of the study showed that the increase in the number of atoms caused changes in spectral of (PVA) which include the shift in some bonds and change in the intensities. Also, from Ultra Violet and Visible spectrum observed that absorption increases by increasing the number of atoms. The total energies decrease with the increase in the number of atoms forming the nanocomposites.

M. Yaqoob, *et al*. in (2020) [45] used first principle calculation of Selenium N-heterocyclic carbene compounds through DFT studies: Synthesis, characterization and biological potential, by using 6-31G (d) level of DFT (Density Functional Theory). Theoretical calculation showed that compounds are highly biologically active, as their synthesis is exigency of the time so these compounds were synthesized. Synthesized compounds were characterized by UV-visible, FT-IR, carbon and proton NMR spectroscopies. Antioxidant and anticancer properties of compounds were calculated and their characteristics were compared with the charactristics of imidazole present in the literature and the results were the almost same as calculated by the theoretical method.

H. Ahmed, *et al.* in (2020) [46] it was studied the determination of optical parameters of films of PVA/TiO_2/SiC and PVA/MgO/SiC nanocomposites for optoelectronics and UV-Detectors, by using the Gaussian 0.9 and Gaussian view 5.0.8 programs on the basis of the density functional theory at B3LYP level with 6–31 G basis set. The results of the study showed that the both nanocomposites have high absorbance in the UV region and have indirect energy gaps 1 eV < Eg < 2.2 eV.

W. Qu, *et al*. in (2020) [47] in this research, it was studied DFT studies of adsorption and interactions between selenium species and mercury on activated carbon, by using density functional theory calculation. The results of the study showed that the spin multiplicity of the systems was considered to determine optimal structures. The frequency, density and other calculations were carried out by using Multiwfn to obtain theoretical parameters after the geometry optimization.

M. Ali, *et al*. in (2021) [48] it was studied the computational screening of structural, electronic, and optical properties for SiC, $Si_{0.94}Sn_{0.06}C$, and $Si_{0.88}Sn_{0.12}C$ lead-free photovoltaic inverters using DFT functional of the first principle approach, by using DFT based on CASTEP code. Studied the electronic, structural, and optical properties of hexagonal SiC and density of states. The results of the study showed that the doping effect of 12% of Sn metals on silicon carbide (SiC) can reduce the band gap reached 1.65 eV.

H. Ahmed and A. Hashim, in (2021) [49] calculated the structural, optical and electronic properties of silicon carbide doped PVA/NiO for low cost electronics applications, by using the Gaussian 0.9 software with the assistance of Gaussian View 0.5 and DFT with the (LanL2DZ). The study's findings indicated that the UV-Vis spectra of tiny molecules are more intense than those of bigger molecules and move near the cutoff energy frequency for large molecules. Additionally, when the number of atoms increases, the energy gap, cohesive energy, and ionization potential decrease.

1.9 Aims of the Work

The general objective of this work is study of the structural, spectroscopic and electronic properties of (PVA-SeO_2-SiC) by using Gaussian program and density functional theory method with hybrid functional (B3LYP) and (LanL2DZ) basis sets.

The investigated properties include energy gap, bond lengths, highest occupied molecular orbital (HOMO), lowest unoccupied molecular orbital (LUMO), Ultraviolet–visible spectra (UV-Vis) and nuclear magnetic resonance spectra (NMR). Vibrational properties include infrared and Raman spectroscopy.

Chapter Two

Mathematical and Programming Part

2.1 Introduction

Computational chemists and physicists can employ four main methods: they are molecular mechanics (MM) methods, Semi empirical (SE) methods, ab initio methods and density functional theory (DFT) methods [50].

Density functional methods form the basis of a diversified and very active area of present day's computational atomic, molecular, solid state and even nuclear physics. A large number of computational physicists use these methods because of their tremendous success. In the seventies (Thomas-Fermi theory), the eighties (Hohenberg-Kohn theory), and density functional concepts became subjects of mathematical physics [51]. Questions commonly investigated by computational chemistry include molecular geometries, energies of molecules, chemical reactivity, IR, UV, NMR spectra, and the physical properties of substances [52].

2.2 Schrödinger Equation

The basis for studies of the electronic structure of materials is the time-independent Schrödinger equation. The state of any system is described by the wave function (Ψ), which in turn depends on the electrons and nuclei positions in the system [53]. This wave function is computed by solving the Schrödinger equation numerically or mathematically, and the solution gives the total energy of the system and some physical properties. This equation is represented as follows [54,55]:

$$\hat{H}\Psi = E\Psi \qquad (2.1)$$

Where $\hat{H}$ is the Hamiltonian operator, Ψ is the wave function of all participating particles, and E is the total energy of the particle.

The Hamiltonian operator is given by:

$$\hat{H} = \hat{T} + \hat{V} \tag{2.2}$$

Here, $\hat{T}$ is the kinetic energy operator and $\hat{V}$ is the potential energy operator.

$$\hat{T} = \frac{1}{2m}\left(\hat{P}_x^2 + \hat{P}_y^2 + \hat{P}_z^2\right) \tag{2.3}$$

where $\hat{P}$ is the linear momentum operator and m is the particle mass.

$$\hat{P}_x = -i\hbar\,\frac{\partial}{\partial x}\,. \qquad \hat{P}_y = -i\hbar\frac{\partial}{\partial y}\,. \qquad \hat{P}_Z = -i\hbar\frac{\partial}{\partial z} \tag{2.4}$$

By substituting equation (2.4) in the equation (2.3), the result is:

$$\hat{T} = \frac{-\hbar^2}{2m}\nabla^2 \tag{2.5}$$

Where $\nabla^2 = \frac{\partial^2}{\partial x^2} + \frac{\partial^2}{\partial y^2} + \frac{\partial^2}{\partial z^2}$ is the Laplacian operator.

Substituting equations (2.2) and (2.5) in equation (2.1) yields [56]:

$$\left[\frac{-\hbar^2}{2m}\nabla^2 + \hat{V}\right]\Psi = E\Psi \tag{2.6}$$

A central problem in quantum mechanical calculations is to solve the time-independent Schrödinger equation [57]. The Schrödinger equation can be solved exactly only for the simplest systems. In quantum mechanical calculations, one is often concerned with larger systems and the problem must thus be reduced to approximate solutions to the equation [58].

2.3 The Wave Function

The wave function Ψ is not physically observable, but its square $[\Psi]^2$ can be interpreted as the probability density, which yields a probability when multiplied by the volume of a region. The acceptable wave function for a system has to be orthogonal to each other, normalized (orthonormal), and form a complete set.

‘‘Orthonormality’’ means that the wave functions have the property:

$$\int \Psi_i^{*}\, \Psi_j dx_N = \langle \Psi_i | \Psi_j \rangle = \delta_{ij} = \begin{cases} 1, & if \quad i = j \\ 0, & if \quad i \neq j \end{cases} \tag{2.7}$$

Completeness means that the ‘‘delta function’’ which is the sharpest possible function of the unit area can be constructed from the complete set of eigen functions [59]. The energy of a wave function can be calculated as an expectation value of the Hamiltonian operator:

$$E = < \hat{H} > = \frac{\int \Psi^{*} \hat{H} \Psi \, dt}{\int \Psi^{*} \Psi \, dt} \tag{2.8}$$

The wave function Ψ describes a many particle system [60].

2.4 The Born Oppenheimer Approximation

The reparability of nuclear and electronic motion was formulated in 1927 by Born and Oppenheimer by means of a precise but rather complex mathematical analysis. A molecule contains both nuclei and electrons, but nuclear and electronic motions may be considered separately because the nuclei are much heavier than the electrons and their motion is therefore more restricted [61]. The reparability of nuclear and electronic motion is known as the Born-Oppenheimer Approximation. So the wave function of a molecule could be divided into:

$$\Psi_{\text{total}} = \Psi_{\text{electron}} \times \Psi_{\text{nucleus}} \quad (2.9)$$

$$\Psi = \Psi_{\text{e}}(\text{R.r})\,\Psi_{\text{n}}(\text{R}) \quad (2.10)$$

The kinetic energy of nuclei and the potential energy of nuclei-nuclei can be eliminated from the Hamiltonian operator, and the Hamiltonian operator $\hat{\text{H}}$ is simplified as the following:

$$\hat{H} = \hat{T}_e + \hat{V}_{ne} + \hat{V}_{ee} \quad (2.11)$$

In the easy equation only three energy operators are left. They are electron kinetic energy operator $\hat{\text{T}}_{\text{e}}$, electron-nuclear interaction energy operator $\hat{\text{V}}_{\text{ne}}$ and electron-electron interaction energy operator $\hat{\text{V}}_{ee}$. The system can actually be described as all electrons moving in a potential field of nuclei with fixed positions [62,63].

2.5 Hartree - Fock (HF) Theory

Hartree-Fock is one of the most important approximation used to solve the Schrödinger equation for all electrons in systems. It is the basis of molecular orbital (MO) theory; this means that each electron's motion can be described by a single-particle function (orbital) which does not depend explicitly on the instantaneous motions of the other electrons [52].

Hartree assumed that the total wave function could be generally approximated as a series of one electron wave function [64]. The so-called the Hartree – Fock equations:

$$\hat{\text{f}}_{\text{i}}\,\Psi_{\text{i}} = \varepsilon_{\text{i}}\Psi_{\text{i}} \quad (2.12)$$

Where Ψ_i is an eigenfunction of the operator $\hat{f}_i$, which is also known as the Fock operator and ε_i is the corresponding energy.

the approximate energies calculated are all equal to or greater than the exact energy. The energies are calculated in units called Hartrees (1 Hartree = 27.2116 eV) [65]. The Hartree-Fock approximation approach posits that the wave function of a system of (n electrons) may be expressed by Slater determinant. This determinant is a statement that the spin of all the electrons obeys Pauli Exclusion Principle. The wave function of Hartree-Fock is commonly modeled as a Slater determinant.

$$\Psi\,(1.2.\ldots.n) = \frac{1}{\sqrt{n!}}\begin{vmatrix} \Psi_1(\chi_1) & \Psi_2(\chi_1) & \ldots & \Psi_n(\chi_1) \\ \Psi_1(\chi_2) & \Psi_2(\chi_2) & \ldots & \Psi_n(\chi_2) \\ \vdots & \vdots & \ddots & \vdots \\ \Psi_1(\chi_n) & \Psi_1(\chi_n) & \ldots & \Psi_n(\chi_n) \end{vmatrix} \qquad (2.13)$$

where Ψ is the electronic wave function, and $\frac{1}{\sqrt{n!}}$ is a normalization factor [52].

2.6 Density Functional Theory (DFT)

Density functional theory is one of the most popular and successful quantum mechanical approaches to computing the electronic structure of matter [66].

In 1927, the functional predecessor to density theory was the Thomas-Fermi model, developed by Thomas and Fermi. Thomas and Fermi are calculated the energy of an atom by representing its kinetic energy as a function of the electron density. DFT predicts a great variety of molecular properties; molecular structures, vibrational frequencies, ionization energies, electric, atomization energies, reaction paths, and magnetic properties, etc. [64, 67].

DFT methods are becoming more and more popular because of the results obtained are comparable to the ones obtained by using ab initio methods because of the drastically reduced CPU time. The DFT method differs from other methods which are based on HF calculations in the way that it is the electron density that is used to compute the energy instead of a wave function [68, 69].

DFT calculates the characteristics of a large number of particles as a function of their electron density ρ(r). The electron density of a given state is defined as the number of electrons per unit volume. It is reliant on only three coordinates regardless of the system's number of electrons, as follows [70]:

$$N = \int \rho(\vec{r})\, d\vec{r} \qquad (2.14)$$

The electron density is defined as the possibility of finding an electron(s) in a given region, and when the distance between the electron and the nucleus approaches infinity, it approaches zero. As the number of electrons rises, theoretically speaking, the wave function approaches get substantially more difficult [71].

The fundamental concepts of DFT rely on the ground state energy and all other ground state electronic properties are uniquely determined by the electron density. Furthermore, the exact ground state of the system corresponds to the electronic density for minimal total energy [70].

2.6.1 Hohenberg-Kohn Theory

Hohenberg-Kohn results reduced the problem of solving the many body Schrödinger equation to the problem of minimizing a density functional, They proved that in 1964 a many electron system of the ground state can be determined by the ground state electron density ρ(r) [64, 66, 72].

Theorem I: The ground state energy of a many-electron system is a unique, universal functional of ground state electron density ρ(r).

Theorem II: The functional of ground state energy is minimized by the ground state electron density ρ(r) for a many-electron system.

Any ground state properties (according to these theorems) of a many electron system can be expressed in terms of the ground state electron density ρ(r). The ground state energy functional E_V can be described as:

$$E_V[\rho] = \int \rho(\vec{r})\, V_{ext}(\vec{r}) d\vec{r} + F_{HK}[\rho] \quad (2.15)$$

Where $\hat{V}_{ext}$ is the external potential, and F_{HK} is a functional of the electron density ρ(r) to be determined which includes kinetic energy and all the electron-electron interactions [73, 74]:

$$F_{HK}[\rho] = T[\rho] + E_{NC}[\rho] + J[\rho] \quad (2.16)$$

Where $T[\rho]$ is the kinetic energy, $E_{NC}[\rho]$ is the non-classical electron–electron interaction energy, and $J[\rho]$ is the classical Coulomb energy.

HK theorem assumes that F_{HK} exists, but the actual form of F_{HK} is not known and must be approximated [75].

2.6.2 Kohn-Sham Equations

In the real system with the ground state density ρ(r) there exists a noninteracting system with the same ρ(r).

Equation (2,16) can rewrite as [76]:

$$F[\rho] = T_S[\rho] + J[\rho] + E_{NC}[\rho] \quad (2.17)$$

where $T_S[\rho]$ is the Kinetic energy of noninteracting electron system. The electron density of noninteracting system is described by a single Slater determinant of orbitals.

The DFT exchange–correlation energy $E_{xc}[\rho]$ of interacting electron system can be defined in the form:

$$E_{xc}[\rho] = T[\rho] - T_S[\rho] + E_{NC}[\rho] \tag{2.18}$$

$$V_{xc}(r) = \frac{\delta E_{xc}[\rho]}{\delta \rho_{(r)}} \tag{2.19}$$

Where $V_{xc}(r)$ is the exchange – correlation potential.

Equation (2,19) known as the Kohn-Sham equation, is formally exact and contain only one unknown term, $E_{xc}[\rho]$. Kohn–Sham approach is the famous work that was embraced in many purposes [75, 77].

The physics of Kohn-Sham equation is unlike that of Schrödinger equation. The significance of Kohn-Sham equations consists that, it reduced an interacting many-body problem to a set of independent equations which describes the state of single electron in the effective potential of other electrons.

The major problem of DFT is to find the exchange-correlation energy (E_{XC}), used so far as a mathematical term. This term includes all the effects of exchange and correlation interactions, such as Pauli exclusion between electrons with same spin orientations, and the instantaneous reaction of electrons with opposite spins. If the exact exchange-correlation function is known, the system is solved exactly. As previously noted, this function is from the difference of the Hamiltonian between the interacting many-electron systems and the non-interacting single electron system [70].

2.6.3 Local Spin Density Approximation (LSDA)

The oldest, simplest and probably the most important functional is the local density approximation (LDA), which was proposed by Hohenberg and Kohn in their original DFT paper. The LDA consists of locally approximating the true exchange-correlation energy of a system by the exchange-correlation energy associated with a homogeneous electron gas and E_{xc} [ρ(r)] depends only upon the local value of electron density. The LDA is only dependent on the local density [78].

While the LSDA does not offer the very exact energy data that many computational chemists demand, it yields more precise results than HF for some characteristics like as equilibrium structures, vibrational frequencies, and dipole moments. In general, the LSDA provides credible data for systems that closely resemble a uniform electron gas with a slowly changing density with the placement. But, electron densities in atomic and molecular systems are not uniform. Consequently, more advanced models are necessary [73].

$$E_{xc}^{LDA}[\rho] = \int \rho(\vec{r})\varepsilon_{xc}\left(\rho(\vec{r})\right)d\vec{r} \tag{2.20}$$

$$E_{xc}^{LSDA}\left[\rho_{\alpha}.\rho_{\beta}\right] = \int \rho(\vec{r})\varepsilon_{xc}\left(\rho(\vec{r})_{\alpha}.\rho(\vec{r})_{\beta}\right)d\vec{r} \tag{2.21}$$

2.6.4 The General Gradient Approximation (GGA)

For the exchange-correlation energy, generalized gradient approximations (GGA's) improve upon the local spin density (LSD) description of atoms, molecules, and solids. We propose an easy derivation of a basic GGA in which all parameters are fundamental constants (excluding those in LSD) [75].

This functional is typically considered superior to the LSDA because it represents the change in density with location. To make the problem easier, (E_{XC}) is usually expressed as the sum of exchange (E_X) and correlation (E_C) terms [73]:

$$E_{xc} = E_x + E_c \tag{2.22}$$

$$E_{xc}^{GGA}[\rho_\alpha . \rho_\beta] = \int f\left(\rho_\alpha \cdot \rho_\beta . \nabla_{\rho_\alpha} \cdot \nabla_{\rho_\beta}\right) d\vec{r} \tag{2.23}$$

The exchange-energy functional may then be acquired by replacing Kohn-Sham orbitals for the HF orbitals in the HF exchange term, and approximate solutions for E_C are searched. Diverse exchange and correlation functionals have been separately developed and can be integrated in a variety of ways. For example, BLYP, which combines Becke's 1988 exchange functional with the Lee-Yang-Parr correlation functional, is a common GGA functional [52].

2.6.5 The Hybrid Functional

This is the most popular DFT model. This method is called to be a hybrid, because it uses corrections for both gradient and exchange correlations. B3LYP, the most widely used hybrid functional, utilizes Becke's 1988 exchange functional (E_X^{B88}) and Lee, Yang, and Parr's correlation functional (E_C^{LYP}) as adjustments to the LSDA exchange and correlation functionals through gradients.

The hybrids functional are very successful in describing a wide range of molecular properties accurately. In large molecules and solids, however, calculating the exact (Hartree-Fock) exchange is computationally expensive, especially for systems with metallic characteristics [78, 79].

$$E_{xc}^{B3LYP} = (1-a)E_x^{LSDA} + aE_{xc}^{HF} + bE_x^{B88} + cE_c^{LYP} + (1-c)E_c^{LSDA} \tag{2.24}$$

2.7 Basis Sets

A basis set is a set of functions used to describe the shape of the orbitals in an atom. Molecular orbitals and entire wave functions are created by taking linear combinations of basis functions and angular functions. Most semiempirical methods use a predefined basis set. When ab initio or density functional theory calculations are done, a basis set must be specified although it is possible to create a basis set from scratch, most calculations are done using existing basis sets. The type of calculation performed and basis set chosen are the two biggest factors in determining the accuracy of results [62, 80].

2.7.1 Slater Type Orbitals (STOs)

It seems to be the natural choice for basis functions. They are exponential that mimic the exact eigen functions of the hydrogen atom.

One of the disadvantages of (STO) is that many –center integrals such as coulomb and HF- exchange terms are difficult to compute with (STO). Therefore, it does not play a role in modern wave function based quantum chemistry codes [61, 75].

2.7.2 Gaussian Type Orbitals (GTOs)

The (GTO) basis function in HF and related methods are popular because very efficient algorithms exist for analytically calculating the many- center integrals. In order to improve the GTO basis sets, one usually employs a contracted GTO basis set in which several primitive Gaussian functions are mixed to give a contracted Gaussian function (CGF) [81, 82].

The tail of the wave nuclei compared with the STO function in the GTO is represented poorly. A rough estimate says that three times as many GTOs as STOs are required in order to reach the same level of accuracy. One of the advantages of

the Gaussian basis set is that the product of two Gaussian functions is another Gaussian function. As a result, for the calculations of Coulomb and HF-exchange terms the analytical solution is available for the Gaussian functions.

The basis sets used in Gaussian are classified into: minimal basis sets, split valence sets, Polarization and Diffuse Functions and others [64, 66, 52].

2.7.2.1Minimal Basis Sets

The minimal basis set is the minimum number of basis functions X needed to describe the ground states of the component atoms (represent all the electrons of each atom) in a molecule. A common name of minimal basis sets is STO- n G, the n (n=2-6) represents the number of Gaussian primitive functions that comprise a single basis function. In these basis sets, the same number of Gaussian primitives comprises core and valence orbitals. Minimal basis sets typically give rough results that are insufficient for research – quality publication, but are much cheaper than their larger counterparts [63, 71, 83, 84].

2.7.2.2 Split-Valence Basis Sets

A split-valence basis sets the inner-shell atomic orbitals are represented by one basis function and the valence orbitals are represented by two or more basis functions (Pople basis sets) [52, 73, 85]. An easy way to broaden a basis set is to expand the number of basis functions used for each orbital. Split-valence basis sets have several basis functions for varying orbital exponents for each valence orbital but just one for each core orbital. The valence double-zeta (VDZ) basis set, for example, utilizes two basis functions per valence orbital, whereas the valence triple-zeta (VTZ) basis set utilizes three.

While split valence basis sets give a more accurate description of molecular orbitals due to their support for varying atom sizes, they are still incapable to provide their own balanced basis set [86].

2.7.2.3 Polarization and Diffuse Functions

To improve the findings, the basis set must include polarization functions [52, 85, 86]. Polarization functions are higher angular momentum functions, such as d- and f-type functions for heavy atoms and p- and d-type functions for hydrogen and helium atoms [87, 88, 89]. This makes the base set more flexible by letting the shape of the orbital change (i.e., become polarized in one direction). Polarization functions are useful in systems involving hydrogen, such as hydrogen bonding and proton transfers, since they allow the s orbital to deviate from its normal spherical form. Polarization functions are frequently utilized because they produce more accurate calculated geometries and vibrational frequencies [87, 90].

The addition of polarization functions is indicated in brackets whereas diffuse functions denoted by '+'. For example, the 6-31++G(d, p) basis set contains functions of the d type for all heavy atoms and functions of the p type for hydrogen and helium. The first '+' denotes the inclusion of diffuse s- and p-type functions on heavy atoms, whereas the second '+' represents the inclusion of diffuse s-type functions on hydrogen [86, 75].

2.8 Electronic Properties

2.8.1 Total Energy (E_{total})

The total energy of a system is the sum of its total kinetic and potential energy, at the optimal structure, the molecule's total energy must be at the lowest value since it is at an equilibrium point which implies that the resultant of the effective forces is zero [90].

2.8.2 Ionization potential (IP)

The ionization potential (IP) of a molecule is the amount of energy necessary to remove an electron from an isolated atom or molecule. It is described as the difference in energy between positive charged energy $E_{(+)}$ and neutral energy $E_{(n)}$ using the following relationship [91]:

$$IP = E_{(+)} - E_{(n)} = -E_{HOMO} \quad (2.25)$$

2.8.3 Electron Affinity (EA)

EA is the energy differential between neutral energy $E_{(n)}$ and negative-charged energy $E_{(-)}$ when one electron is added to the neutral atom to produce a negative ion and is represented as the following relation between neutral energy $E_{(n)}$ and negative charged energy $E_{(-)}$ [92]:

$$EA = E_{(n)} - E_{(-)} = -E_{LUMO} \quad (2.26)$$

2.8.4 Energy gap (E_{gap})

The energy gap refers to the energy difference between the highest occupied molecular orbital (HOMO) and lowest unoccupied molecular orbital (LUMO) according to the Koopmans theorem [84,93]:

$$Eg = E_{LUMO} - E_{HOMO} \quad (2.27)$$

HOMO and LUMO and their resulting energy gap not only determine the way the molecule interacts with other species, but their energy gap helps characterize the chemical reactivity and kinetic stability of the molecule. A molecule with a small energy gap is more polarizable and is generally associated with a high chemical reactivity, low kinetic stability and is also termed as soft molecule [94].

2.8.5 Cohesive energy (E_{coh})

The energy required to separate the material into isolated free atoms is called cohesive energy. To calculate this propriety it is required the value of the total energy of the system (molecule) and the free atoms need to separate it. The cohesive energy E_{coh} is given by [95, 96]:

$$E_{coh} = (E_{tot} / n) - E_{free} \quad (2.28)$$

Where, n: is the number of atoms [97].

2.8.6 Chemical Potential (K)

DFT's basic variation principle is the electronic chemical potential, where the reactivity indicator is related to how the electronic energy E of a molecule varies when the number of electrons N and the external potential vary. According to Parr et al., there exists an electronic chemical potential K for any system including nuclei and electrons.

The electronic chemical potential, denoted by K, is defined as [98]:

$$K = \left[\frac{\partial E}{\partial N}\right]_V \tag{2.29}$$

Where *v* is the potential due to nuclei.

2.8.7 Chemical Hardness (η)

The chemical hardness (η) is a measure of the resistance to charge transfer. The theoretical definition of chemical hardness has been provided by the density functional theory as the second derivative of electronic energy with respect to the number of electrons N, for a constant external potential V(r) [99]:

$$\eta = \frac{1}{2}\left[\frac{\partial^2 \mathrm{E}}{\partial \mathrm{N}^2}\right]_\mathrm{V} = \frac{1}{2}\left[\frac{\partial \mathrm{K}}{\partial \mathrm{N}}\right]_\mathrm{V} = -\frac{1}{2}\left[\frac{\partial \mathrm{X}}{\partial \mathrm{N}}\right]_\mathrm{V} \tag{2.30}$$

Finite difference approximation to chemical hardness gives,

$$\eta = \frac{IP - EA}{2} \tag{2.31}$$

2.8.8 Chemical Softness (S)

The global chemical softness, S, is a property of molecules that measures the extent of chemical reactivity. It is the inverse of the chemical hardness (η) [100]:

$$S = \frac{1}{2\eta} = \left[\frac{\partial^2 N}{\partial E^2}\right]_V = \left[\frac{\partial N}{\partial K}\right]_V \tag{2.32}$$

2.8.9 Electronegativity (χ)

The electronegativity (Pauling describes it as "the ability of an atom in a molecule to draw electrons to itself") may then be defined as the opposite of the electronic chemical potential [81]:

$$\chi = -K = -\left[\frac{\partial E}{\partial N}\right]_V \tag{2.33}$$

R. Mulliken defined electronegativity as the average of the ionization energy and electron affinity as follows [101]:

$$\chi = \frac{(IP + EA)}{2} \tag{2.34}$$

It can be defined as negative value for average of HOMO and LUMO levels of energy, according to Koopmans theorem [52, 102]:

$$\chi = -\frac{(E_{HOMO} + E_{LUMO})}{2} \tag{2.35}$$

2.8.10 Electrophilicity (ω)

Electrophilicity is definition of an index that tests the stability of energy when the device acquires an additional electrical charge from the atmosphere [95]. It can also be characterized as a measure of energy reduction caused by maximum electron flow between donor and acceptor. It is of two types:

- Electrophiles
- Nucleophiles

electrophiles and nucleophiles are those types of chemical species that either donate or accept electrons to form a new chemical bond. Meanwhile, the reaction mechanism occurring between electron donors and acceptors are best described by concepts of electrophile and nucleophile [99].

$$\omega = \frac{\kappa^2}{2\eta} \tag{2.36}$$

Where K chemical potential is associated with the negative of the electronegativity.

2.8.11 dipole moment

If the positive charge center does not coincide with the negative charge center, a molecule has a persistent electric dipole moment. Permanent electric dipole moments in neutral molecules are commonly found in systems that are neutral.

The dipole moment sum is [103]:

$$X = X_x + X_y + X_z \tag{2.37}$$

2.9 Vibrational Properties

2.9.1 Infrared Spectrum

Normal oscillations that are accompanied by changes in dipole moments are active and may be seen in the range of infrared radiation. The vibration of a molecule is modeled by normal modes of the simple harmonic oscillator to absorb and emit the energy. The Infrared (IR) spectrum is electromagnetic radiation in the range $(1-5) \times 10^3$ cm^{-1} [100].

When the N-atoms system absorbs amount of energy, it will oscillate with three degrees of freedom in translation and rotation, and with (3N-6) degrees of freedom in vibration for ring molecules. A system's oscillations are classified into two types of bands: fundamental and nonfundamental oscillation bands [104]. More variations in dipole moments accompany the basic bands, which are classified according to high intensity as stretch, deformation, wagging, twisting, rocking and bending

oscillations. Unfundamental bands, overtones, and hot bands, on the other hand, have a low intensity [105]. The vibration analysis is valid only when the first derivative of the energy with respect to displacement of the atoms is zero. Also, the analysis at transition states and higher order saddle point is valid [106].

2.9.2 UV-Vis. Spectroscopy

Photons of ultraviolet and visible light are energetic enough to promote outer electrons to excite from lower to higher energy levels. Since the energy levels of matter are quantized, only light with the precise amount of energy can cause transitions from one level to another will be absorbed. Ultraviolet (UV) radiation is the range of radiation just below the visible spectrum of light. The range extends between 10 and 400 nanometers. Many molecules absorb ultraviolet or visible radiation.

The energy absorption is normally associated with transitions of the electrons from the bonding orbitals (HOMO) to the anti-bonding orbitals (LUMO). The difference in energy between (HOMO) and (LUMO) lies in the ultraviolet-visible region of the electromagnetic spectrum. The energy, E, carried by any one quanta is proportional to its frequency of oscillation, that is:

$$E = h\nu = \frac{hc}{\lambda} \tag{2.38}$$

Where ν the frequency, λ is the related wavelength, and h is Plank's constant $h = 6.626*10^{-34}$ J.s .

In addition to electronic excitation, the atoms within a molecule can rotate and vibrate with respect to each other. These vibrations and rotations also have discrete energy levels, which can be considered as being packed on top of each electronic level [107].

2.9.3 Raman Spectroscopy

Raman spectroscopy is a spectroscopic technique based on inelastic scattering of monochromatic light, usually from a laser source. Photons of the laser light are absorbed by the sample and then reemitted. The frequency of the reemitted photons is shifted up or down in comparison with original monochromatic frequency, Raman shifted photons can be of either higher or lower energy, depending upon the vibrational state of the molecule under study.

Stokes radiation occurs at lower energy than the Rayleigh radiation, and anti-Stokes radiation has greater energy. The energy increases or decreases is related to the vibrational energy levels in the ground electronic state of the molecule, and as such, the observed Raman shift of the Stokes and anti-Stokes features are a direct measure of the information about the energies of molecular vibrations and rotations are contained in the scattered radiation produced by the Raman effect and these in-turn are depended on the atoms or ions that constitute the molecule, the chemical bonds between them, the symmetry of the structure, and the physicochemical environment [108]. Raman spectroscopy shown in Figure (2.1).

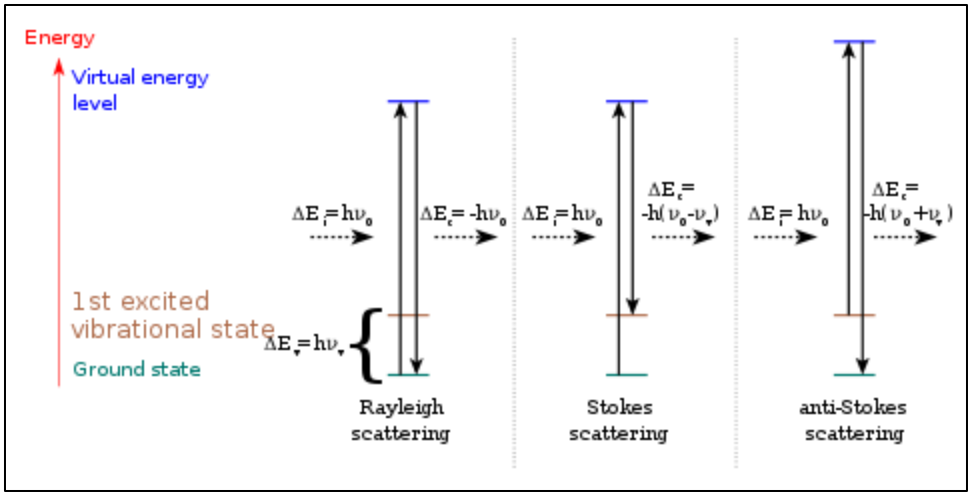

Fig. (2.1): Raman Spectroscopy [109]

2.9.4 Nuclear Magnetic Resonance Spectroscopy (NMR)

Nuclear magnetic resonance spectroscopy, or NMR spectroscopy for short, is a research technique that takes use of the magnetic characteristics of certain atomic nuclei. It establishes the physical and chemical characteristics of atoms or molecules. It is based on the nuclear magnetic resonance phenomenon and may offer extensive information on a molecule's structure, dynamics, reaction state, and chemical environment.

The intermolecular magnetic field around an atom in a molecule alters the resonance frequency, revealing data about the molecule's electronic structure.

NMR spectroscopy is most typically employed by chemists and biochemists to explore the characteristics of organic compounds, even though it is applicable to any material containing spin-containing nuclei. Samples suitable for analysis vary from tiny compounds examined in one dimension using proton or carbon-13 NMR spectroscopy to big proteins or nucleic acids investigated in three or four dimensions. NMR spectroscopy has had a significant influence on the sciences due

to the breadth of information and the diversity of samples, including liquids and solids. When placed in a magnetic field, NMR active nuclei (such as ^{1}H or ^{13}C) absorb electromagnetic radiation at a frequency characteristic of the isotope [110].

2.10 Software

All calculations in this thesis have been performed using the Gaussian09 program packages.

2.10.1 Gaussian Program

Gaussian is a very high quantum chemical software package, available commercially through Gaussian, Inc. The Software runs on virtually all computer platforms, including Microsoft Windows. Additionally, it is accessible via Web-based interface tools such like Web MO. Gaussian program discover by Jone Pople in 1970. Gaussian is the most sophisticated program provided to professors and student researchers via the North Carolina School of Computational Chemistry's computational chemistry site. Gaussian09 (G09) is now available. The "09" relates to the year 2009, when the program was released. G09 is not the latest version [111].

2.10.2 Gaussian View 5.0.8 Program

Gauss view is software that is used to load input files for Gaussian programs and to display the output files for Gaussian programs in the dimensional picture. It is not a calculating program, but it simplifies work with Gaussian programs and provides three significant advantages to users.

First: It lets the user draw molecules of any size, as well as rotate, transfer, and change their size with the mouse.

Second: Gaussian view enables and performs a large number of Gaussian calculations, preparing the complicated input for regular work and sophisticated methods.

Third: The Gaussian view enables the examination of Gaussian computation results through the use of a variety of geometrical techniques, including the following: (Balanced molecular patterns, molecular orbitals, and electronic density surfaces) [112].

Chapter Three

Results and Discussion

3.1 Introduction

This chapter includes the results and discussion of the structural, electronic and spectral properties for (PVA-SeO_2-SiC) nanocomposites.

Gaussian 0.9 program and density functional theory (DFT) are used to calculate many properties. The properties were investigated total energy, energy gap, LUMO, HOMO, cohesive energy, density of states, ionization potential, electron affinity, chemical hardness, chemical softness, and electronegativity. Also, the spectroscopic properties (IR, RAMAN, UV-Vis, NMR) for all molecular systems were investigated at the same level of theory as a function of size variation. Density functional theory (DFT) at the three-parameter hybrid-functional of Beck's 3-parameter exchange with Lee, Yang, and Parr correlations functional (B3LYP) with Los Alamos National Laboratory 2-Double-Z(LanL2DZ) basis sets is used. Geometrical optimization is performed first and followed by electronic properties, frequency and vibrational analysis.

3.2 The Structural Properties of (PVA-SeO_2-SiC) Nanocomposites

The geometrical optimization of nanocomposites was calculated to determines many of its physical and chemical properties. It is necessary to find the relaxation of the nanocomposites, in which the optimized structure of the nanocomposites is the structure a minimum energy. Figures (3.1) - (3.4) show the optimized structures of (PVA) (43Atoms), (PVA-SiC) (45Atoms), (PVA-SeO_2-SiC) (46Atoms) and (PVA-SeO_2-SiC) (90Atoms) nanocomposites in the gas state, were obtained with the DFT method using the three-parameter hybrid-functional of Becke (B3LYP) with (LanL2DZ) basis sets.

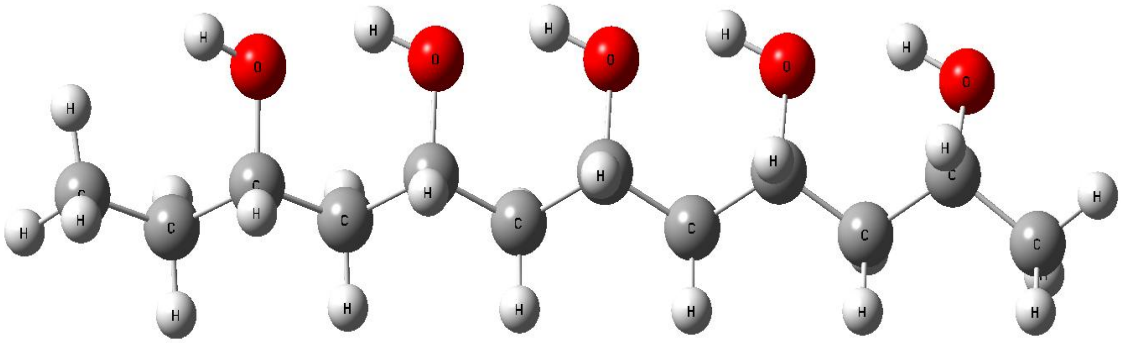

Fig. (3.1): Optimized geometry for (PVA) contains (43 Atoms) at the B3LYP/ LanL2DZ basis set

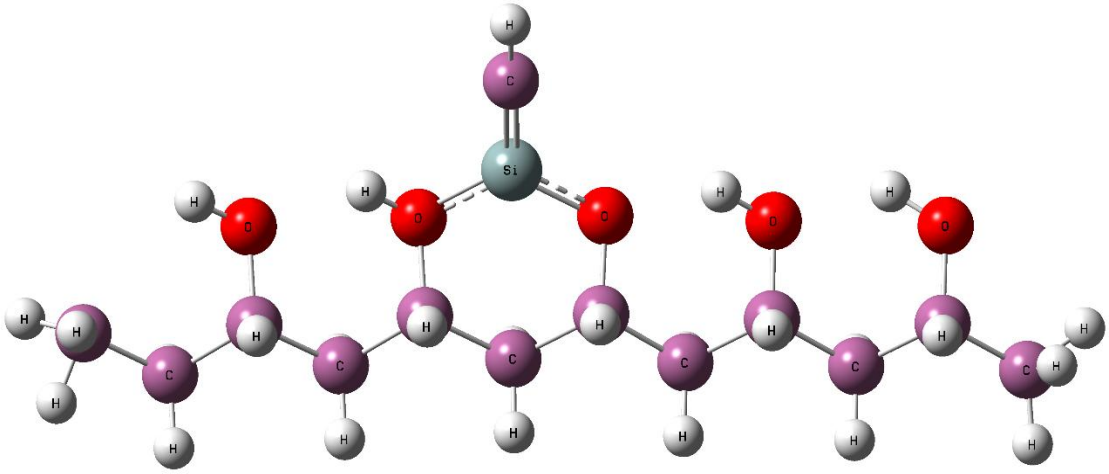

Fig. (3.2): Optimized geometry for (PVA-SiC) contains (45 Atoms) at the B3LYP/ LanL2DZ basis set

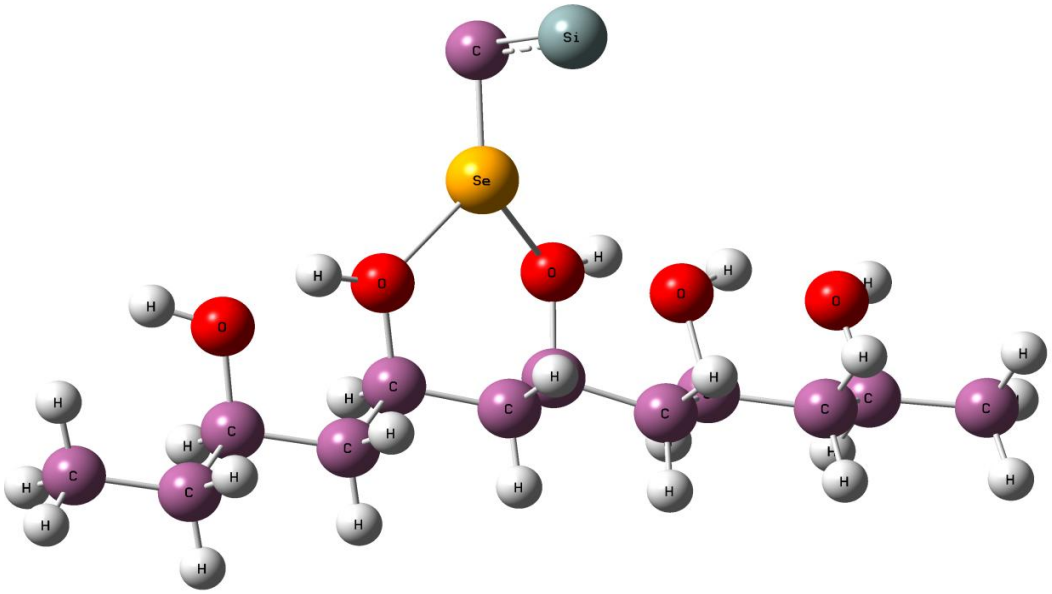

Fig. (3.3): Optimized geometry for (PVA-SeO_2-SiC) contains (46 Atoms) at the B3LYP/ LanL2DZ basis set

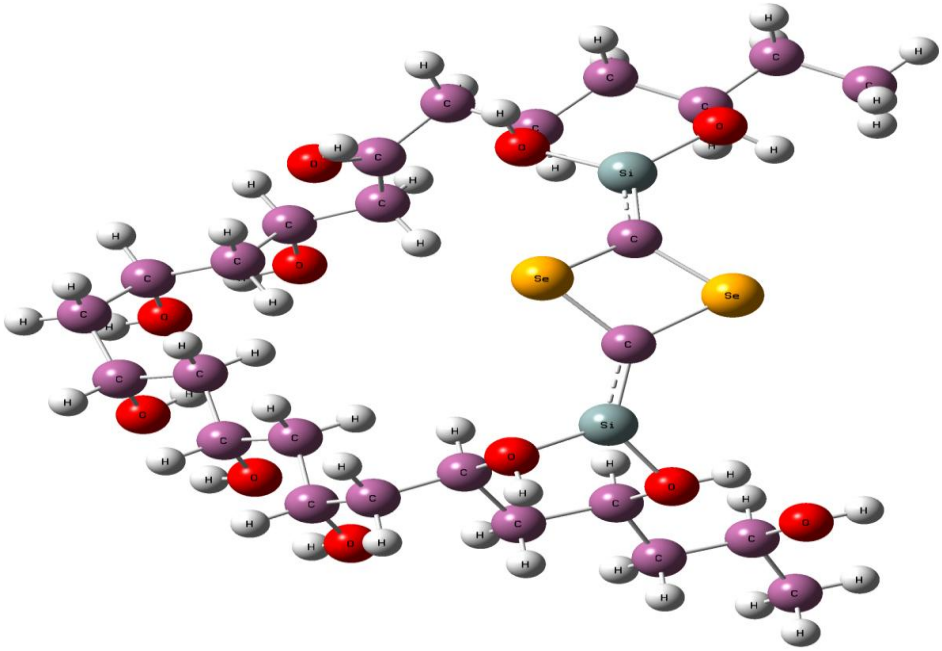

Fig. (3.4): Optimized geometry for (PVA-SeO_2-SiC) contains (90Atoms) at the B3LYP/ LanL2DZ basis set

Table (3.1) shows the geometric parameters of (PVA-SeO_2-SiC) nanocomposites involveing the bond length in Angstrom and bond angle in degree by using the Gaussian 09 package of programs by employing the DFT with the B3LYP/LanL2DZ level, compared to source results [113,114,115].

Table (3.1): The optimized parameters for (PVA-SeO_2-SiC)

Measurements	The optimization parameters	Values
Bonds Å	(C−C)	1.544
	(C−O)	1.483
	(C−H)	1.104
	(O−H)	1.004
	(Se−Si)	2.433
	(Se−C)	1.970
	(C−Si)	1.926
Angles Deg.	(C−C−C)	113.549
	(C−O−H)	108.230
	(Se− Si −C)	52.163
	(O− Se −O)	46.547

3.3 The Spectral Properties of (PVA-SeO_2-SiC) Nanocomposites

3.3.1 The Infrared Spectrum (IR)

IR spectra of (PVA-SeO_2-SiC) nanocomposites results obtained using the Gaussian view 5.0 program and density functional theory (DFT) with (LanL2DZ) basis sets are shown in Figures (3.5) - (3.8). The IR studies of nanocomposites show the interactions in nanocomposites. It shows broad bands at around (3215–3235) cm^{-1} for the samples of nanocomposites are observed due to (O-H) groups in the polymers matrix chain. The bands at (700-1500) cm^{-1} were attributed to the other bonds (C-C) [116,117]. The band at (2901-2907) cm^{-1} is attributed to the (C-H) groups. The bands at (1649-1708) cm^{-1} are assigned to the (C=C) stretching mode. The strong band at (1085-1090) cm^{-1} for the samples of nanocomposites attributed to the stretching mode of (C-O) group. The two strong bands observed at around (1300-1400) cm^{-1} are attributed to the bending and stretching modes of (-CH_2) group [118].

Adding the nanoparticles and increasing the number of atoms caused changes in spectral of (PVA-SeO_2-SiC) nanocomposites which include the shift in some bonds and change in the intensities. These changes are attributed to interactions of SeO_2, SiC nanoparticles with (PVA). The IR studies show that adding nanoparticles leads to the displacement of some of the bonds and not thebemergence of new peaks and this is the basis idea of the nanocomposites. The transmittance in figures decreases slightly with the increase of SiC nanoparticles concentrations which is attributed to increasing the density of nanocomposites [119]. These are consistent with the results of researchers [117,119]. It is observed that when the nanoparticles disperse in the PVA matrix, the FTIR spectra exhibit several irregular shifts related to corresponding bands with changes in intensities of pure PVA [120].

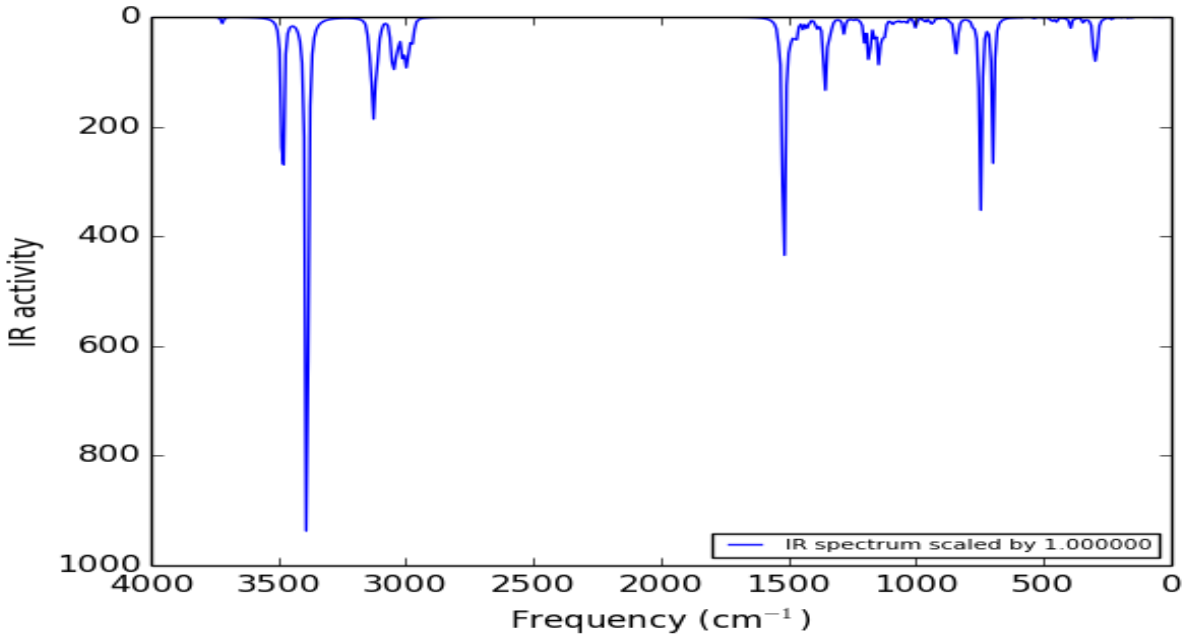

Fig. (3.5): IR spectrum of (PVA) (43Atom) using B3LYP/ LanL2DZ

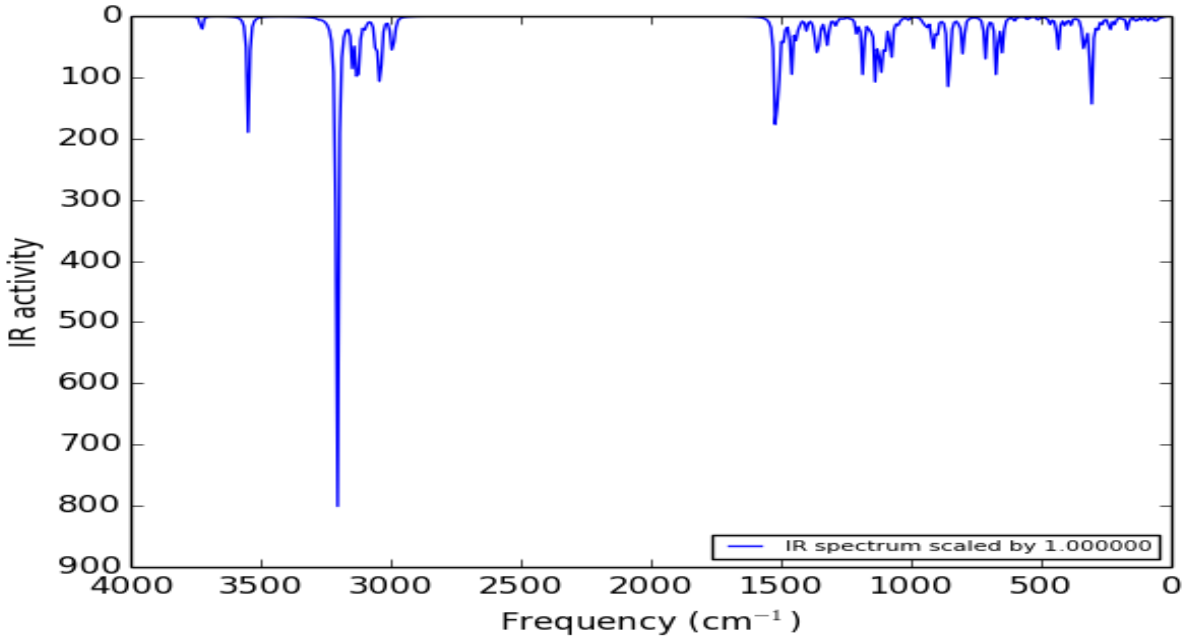

Fig. (3.6): IR spectrum of (PVA-SiC) (45Atoms) using B3LYP/ LanL2DZ

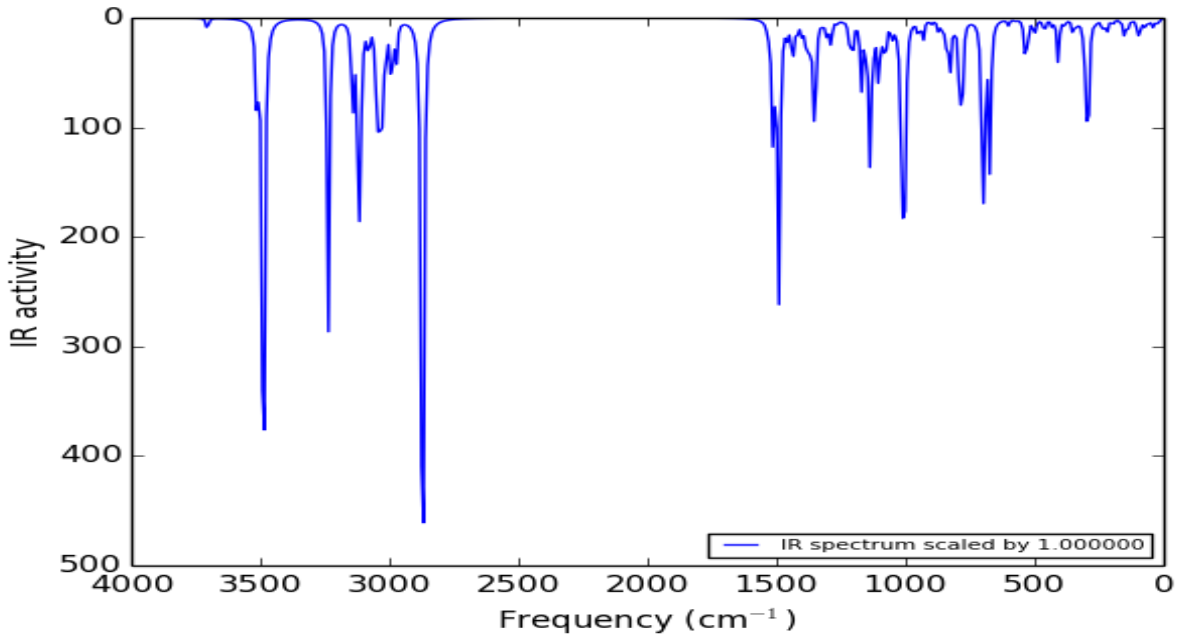

Fig. (3.7): IR spectrum of (PVA-SeO_2-SiC) (46Atoms) using B3LYP/ LanL2DZ

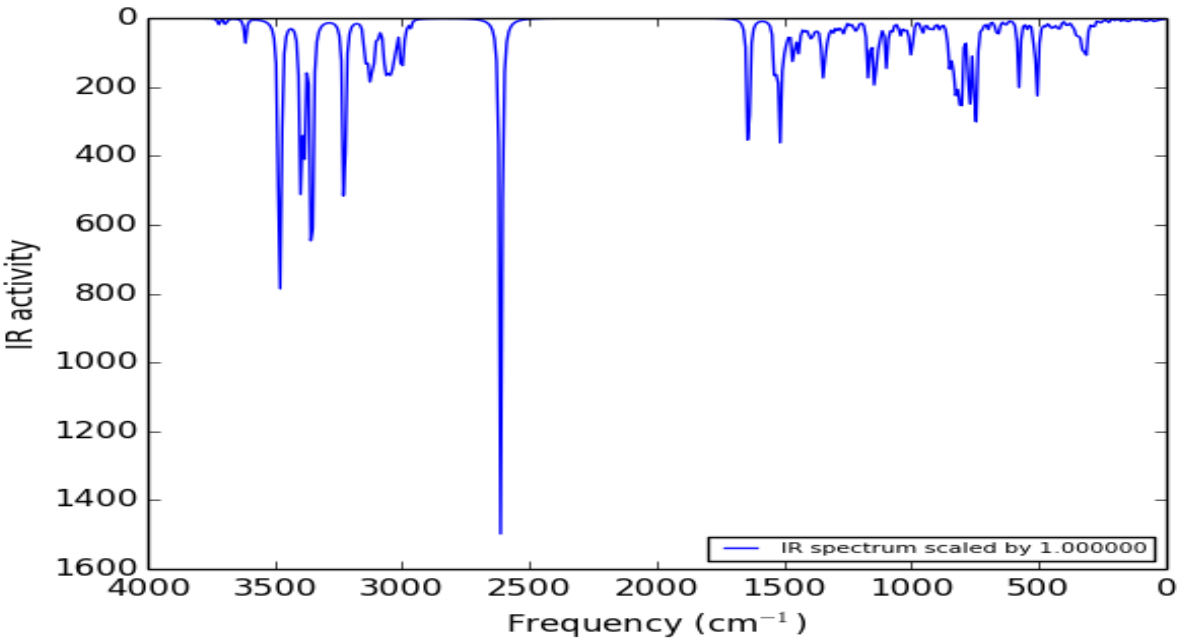

Fig. (3.8): IR spectrum of ((PVA-SeO_2-SiC) (90Atom) using B3LYP/ LanL2DZ

3.3.2 Raman Spectrum

The differences between a Raman spectrum and an infrared spectrum are not surprising. Infrared absorption requires that a vibrational mode of the molecule have a change in dipole moment or charge distribution associated with it. Raman is a very powerful tool for analysis and chemical monitoring**.** Figures (3.9) - (3.12) show the Raman spectrum of (PVA) (43Atoms), (PVA-SiC) (45Atoms), (PVA-SeO_2-SiC) (46Atoms) and (PVA-SeO_2-SiC) (90Atoms) nanocomposites respectively. It shows from the figures that the active region in IR is similar with less activity in Raman**.** The peak intensities in Raman spectrum depend on the probability that a particular wavelength photon will be absorbed. These probabilities can be computed from the wave function by computing the transition dipole moments. This gives relative peak intensities since the calculation does not include the density of the substance. Some types of transitions turn out to have a zero probability due to the molecules' symmetry or the spin of the electrons.

Raman and IR are complementary vibrational spectroscopic techniques. In Raman spectroscopy, a change is observed in the polarization of molecules; that is, visible or ultraviolet photons interacts with the vibrating molecular bonds, gaining or losing part of their energy, thereby generating the spectrum. An advantage of Raman spectroscopy is that the spectral analysis is carried out in reflection mode, so tissues can be probed in their native state without any, or minimal preparation [121,122]. The active region is take place in the range of about (1000-4000) cm^{-1} in all nanocomposites. From figures show the specific bands of nanocomposites that appear with their original characteristics. No significant change or shift of them could be observed.

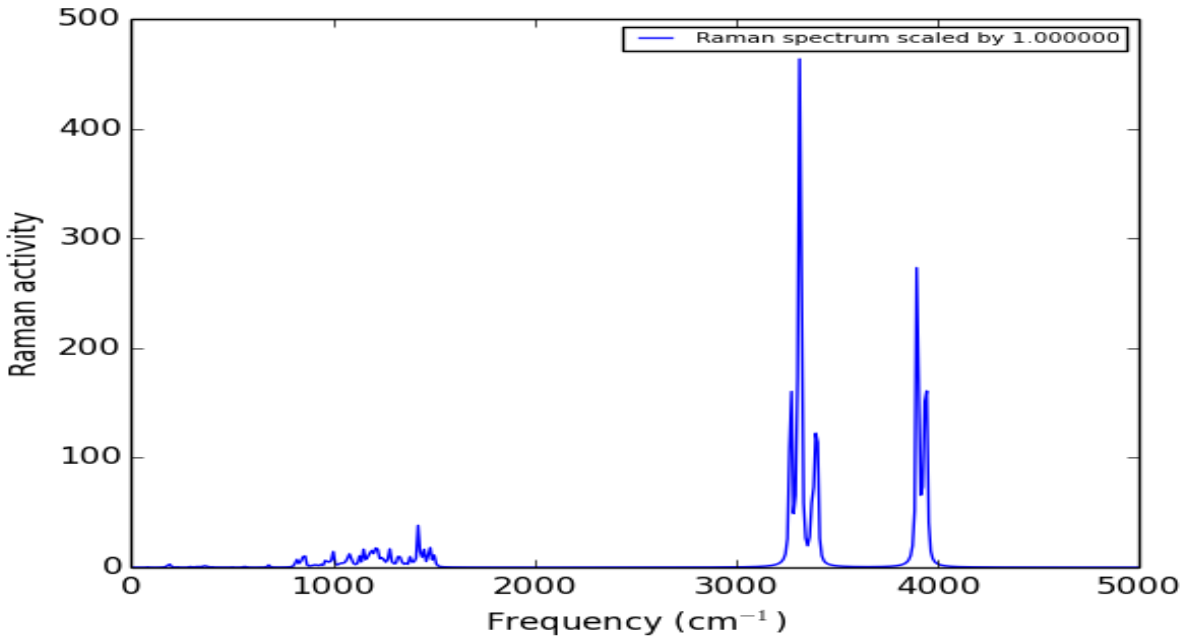

Fig. (3.9): Raman intensities of (PVA) (43 Atoms) as a function of vibration frequency using DFT/ LanL2DZ

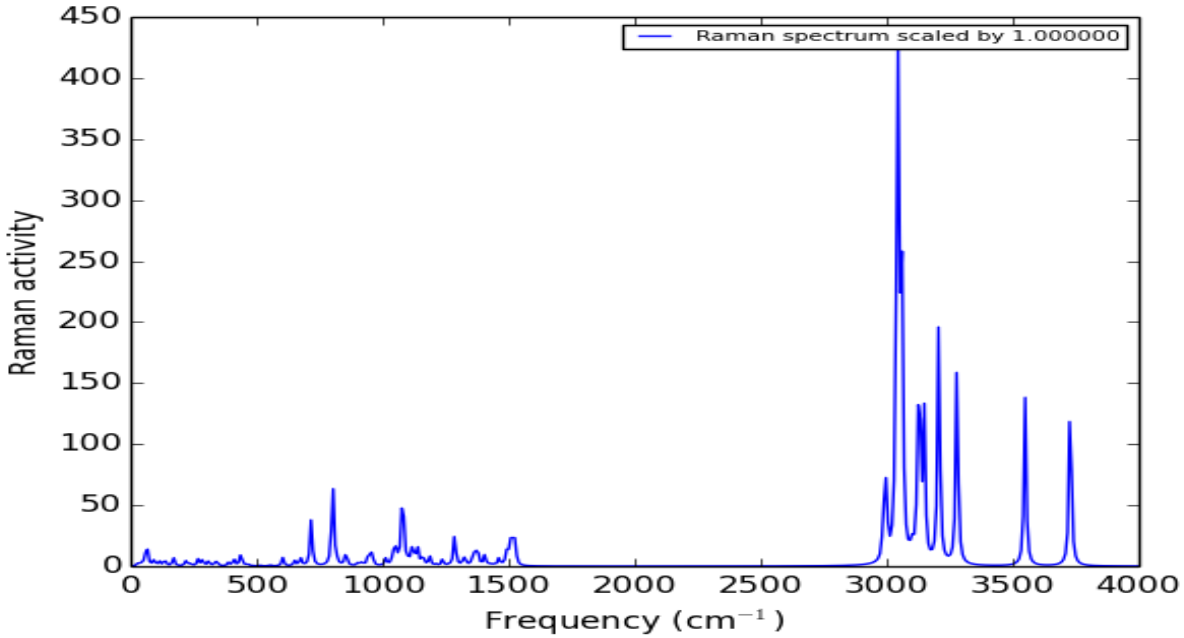

Fig. (3.10): Raman intensities of (PVA-SiC) (45 Atoms) as a function of vibration frequency using DFT/ LanL2DZ

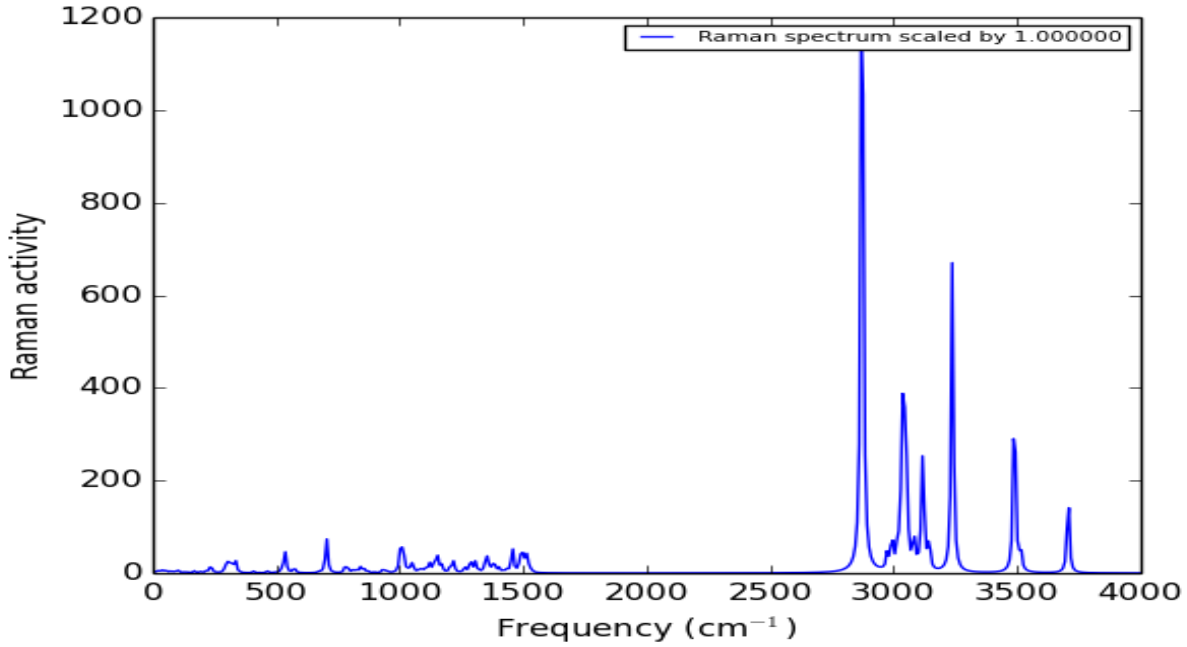

Fig. (3.11): Raman intensities of (PVA- SeO_2-SiC) (46 Atoms) as a function of vibration frequency using DFT/ LanL2DZ

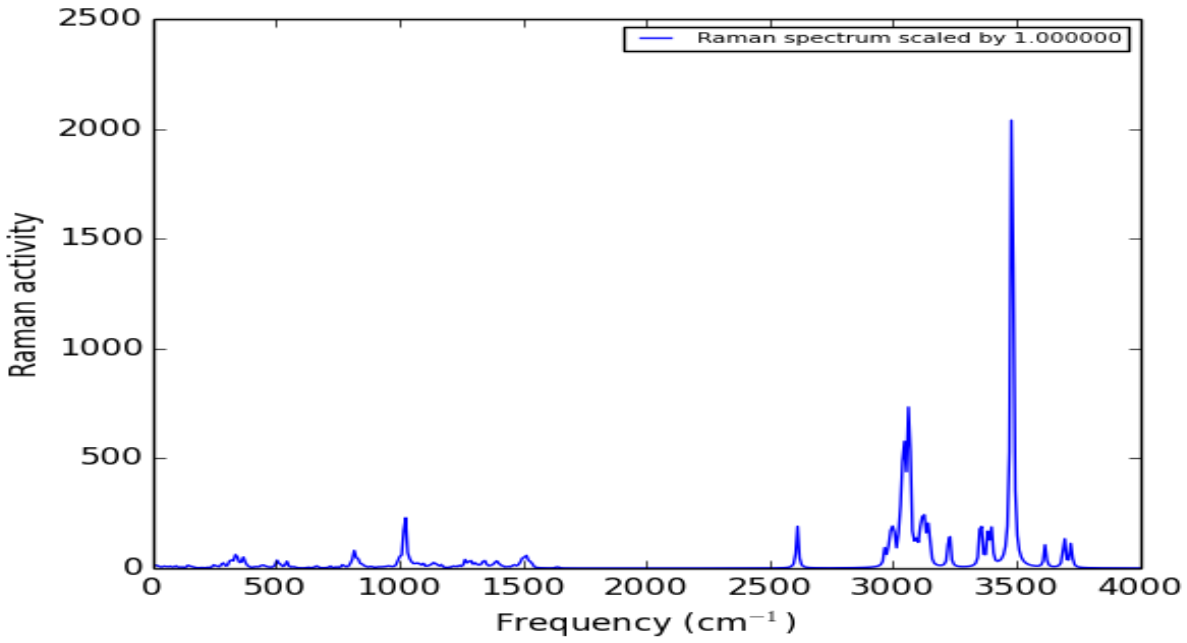

Fig. (3.12): Raman intensities of (PVA- SeO_2-SiC) (90 Atoms) as a function of vibration frequency using DFT/ LanL2DZ

3.3.3 Nuclear Magnetic Resonance (NMR)

Chemical shifts of the structure were calculated at the same level using the Gauge-Included Atomic Orbital (GIAO) approach. Gauge-Independent Atomic Orbital (GIAO) method is used in the present NMR calculations. Absolute isotropic magnetic shielding were transformed into chemical shifts by referencing to the shielding of a standard compound computed at the same level. The chemical shifts were reported in (ppm) for ^{1}H spectra as shown in Figures (3.13) - (3.16) [123].

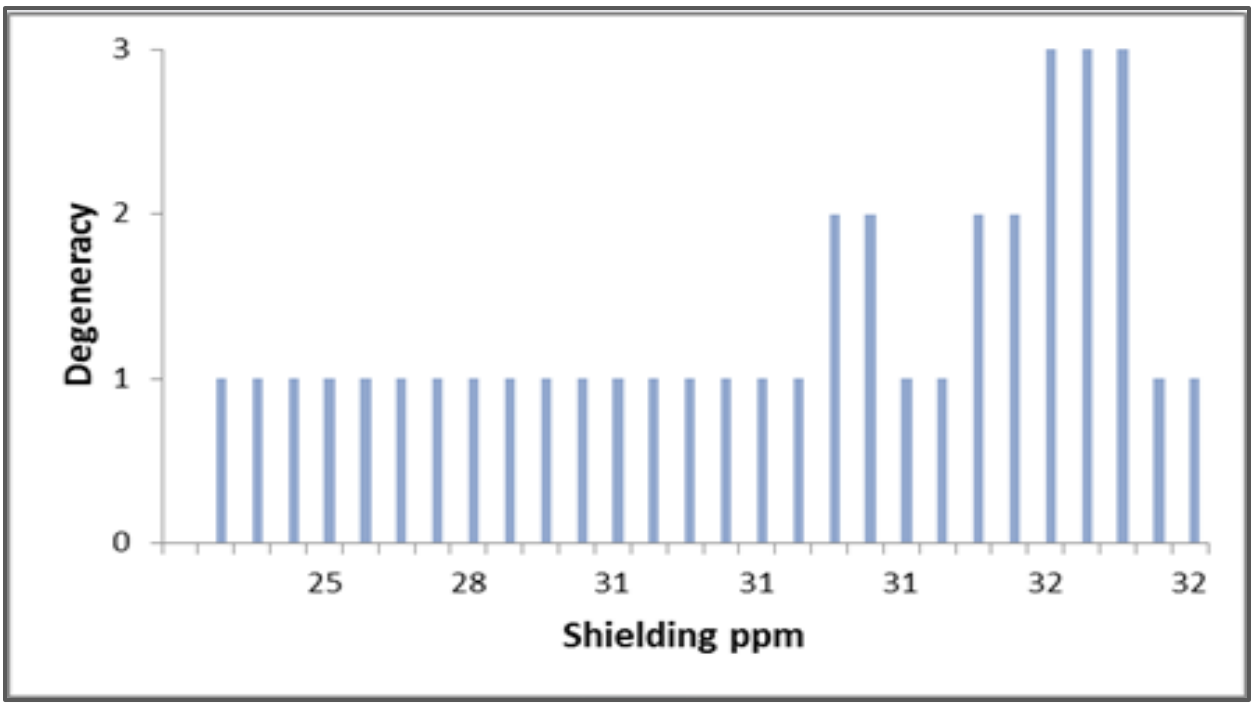

Fig. (3.13): Nuclear Magnetic Resonance of (PVA) (43 Atoms) as a function of vibration frequency using DFT/ LanL2DZ

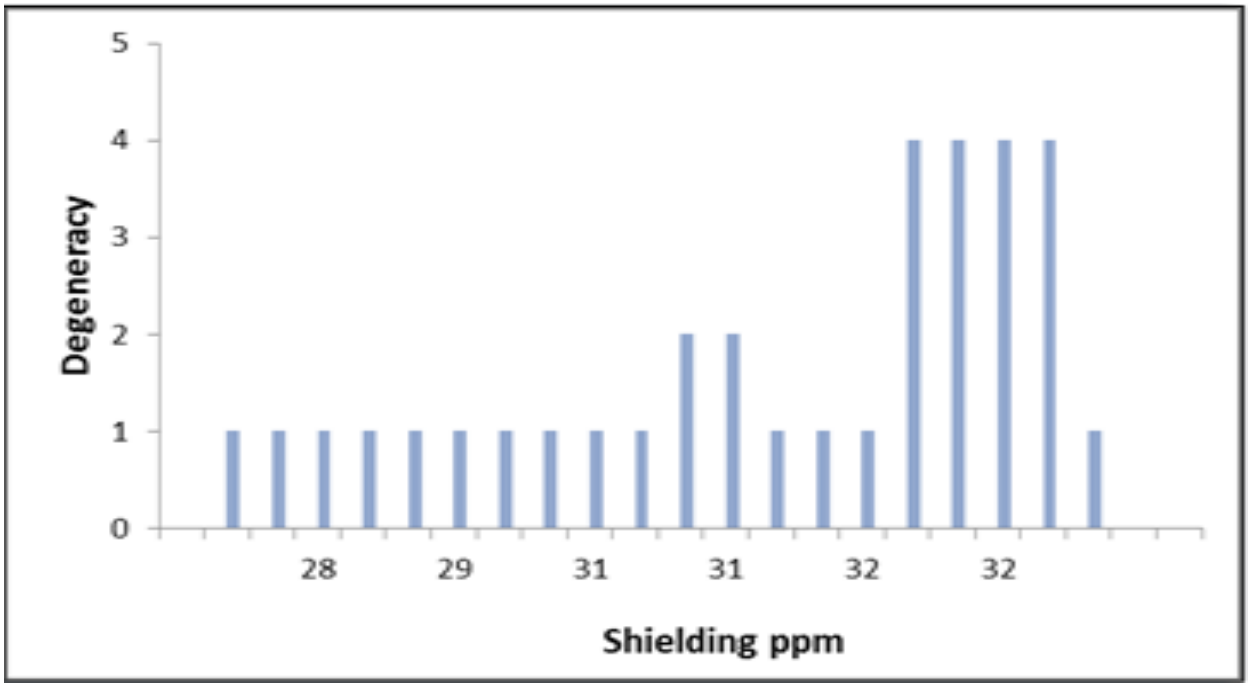

Fig. (3.14): Nuclear Magnetic Resonance of (PVA-SiC) (45 Atoms) as a function of vibration frequency using DFT/ LanL2DZ

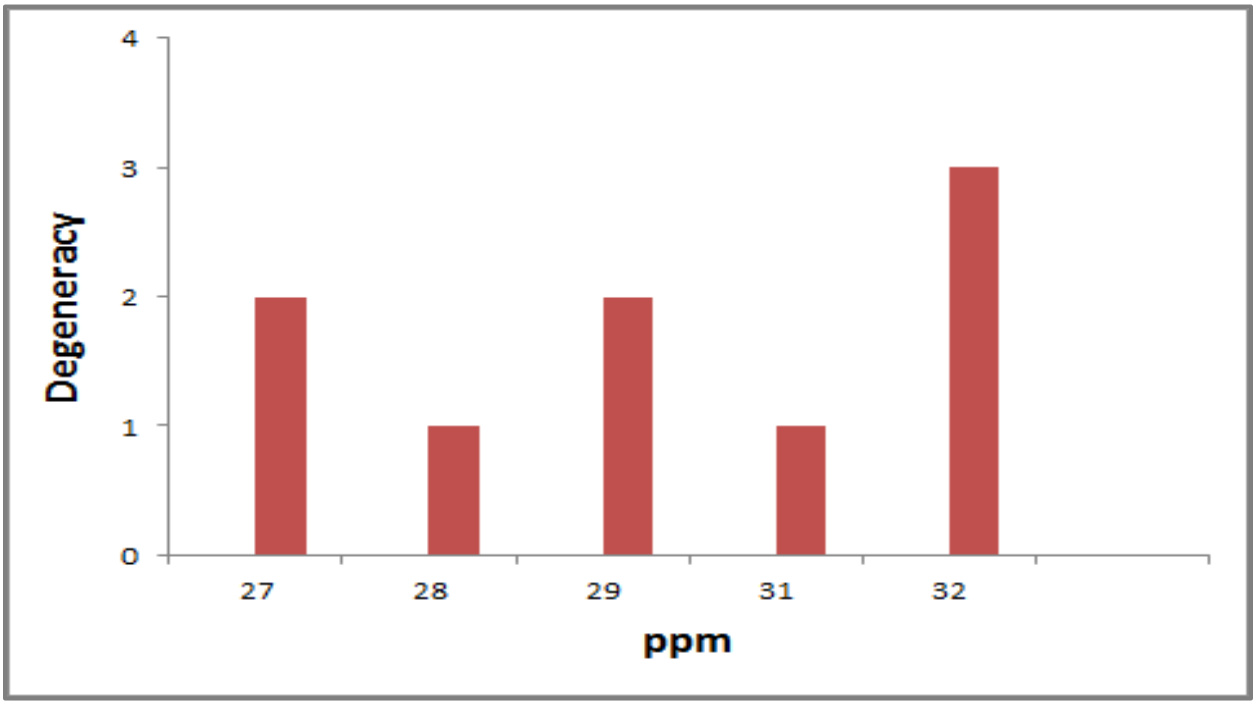

Fig. (3.15): Nuclear Magnetic Resonance of (PVA- SeO_2-SiC) (46 Atoms) as a function of vibration frequency using DFT/ LanL2DZ

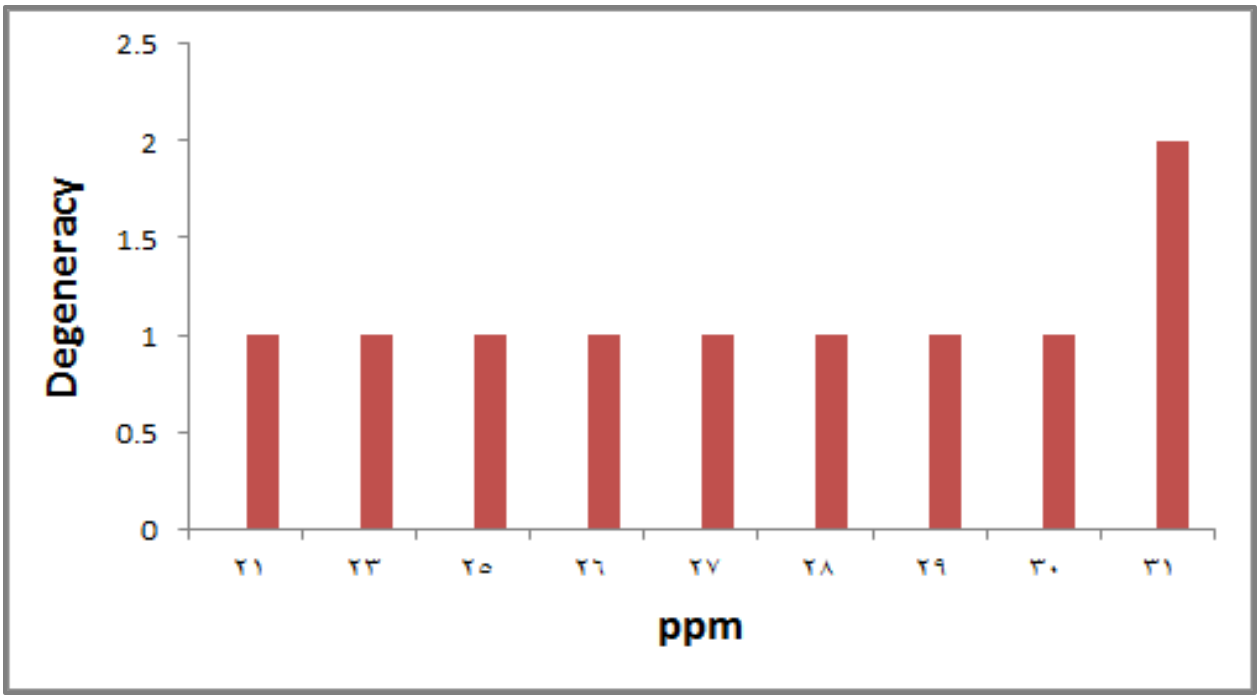

Fig. (3.16): Nuclear Magnetic Resonance of (PVA- SeO_2-SiC) (90 Atoms) as a function of vibration frequency using DFT/ LanL2DZ

3.3.4 Ultra Violet and Visible spectrum

Ultra Violet and Visible spectrum is dependent upon the electronic structure of the molecule. Figures (3.17) - (3.20) Show the UV-Vis spectra that obtained by using Gaussian 09 program and Gaussian view 5.0.8 program and (B3LYP) level with (LanL2DZ) basis sets. The figures show that the spectrum within the limits Ultraviolet-Visible (UV-Vis) of the spectrum for (PVA- SeO_2-SiC) (46 Atoms) and (90 Atoms).

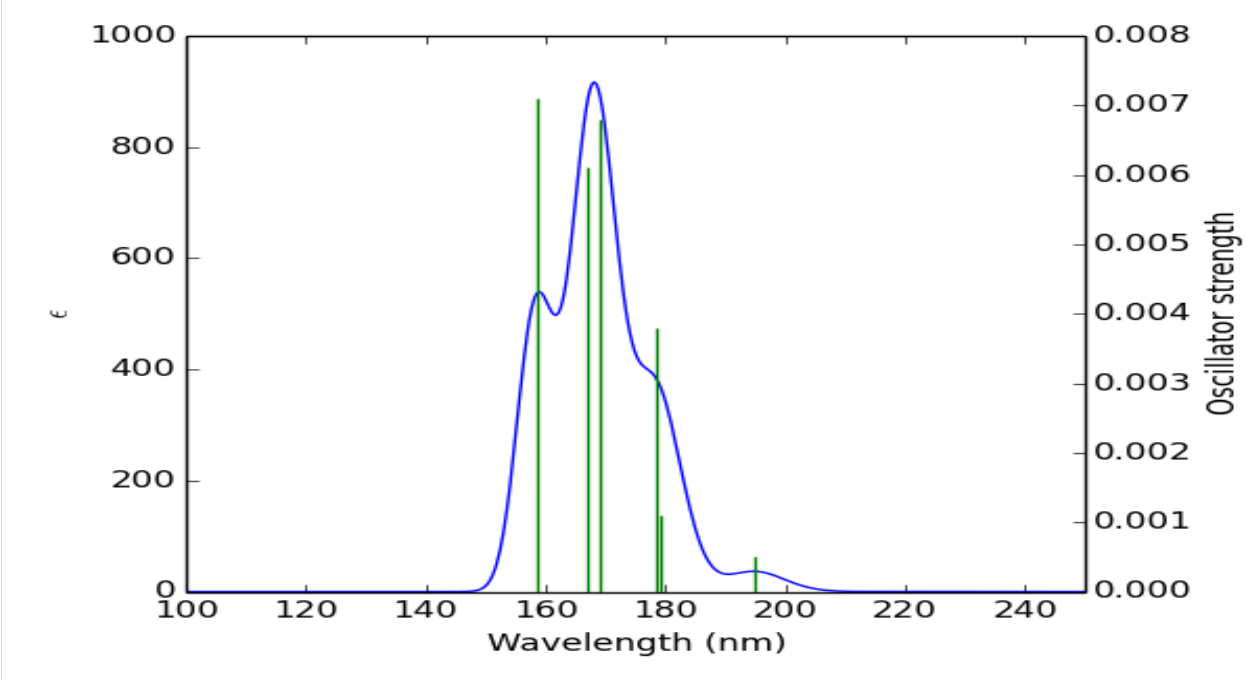

Fig. (3.17): UV-Vis spectrum for (PVA) (43 Atoms) using B3LYP/ LanL2DZ

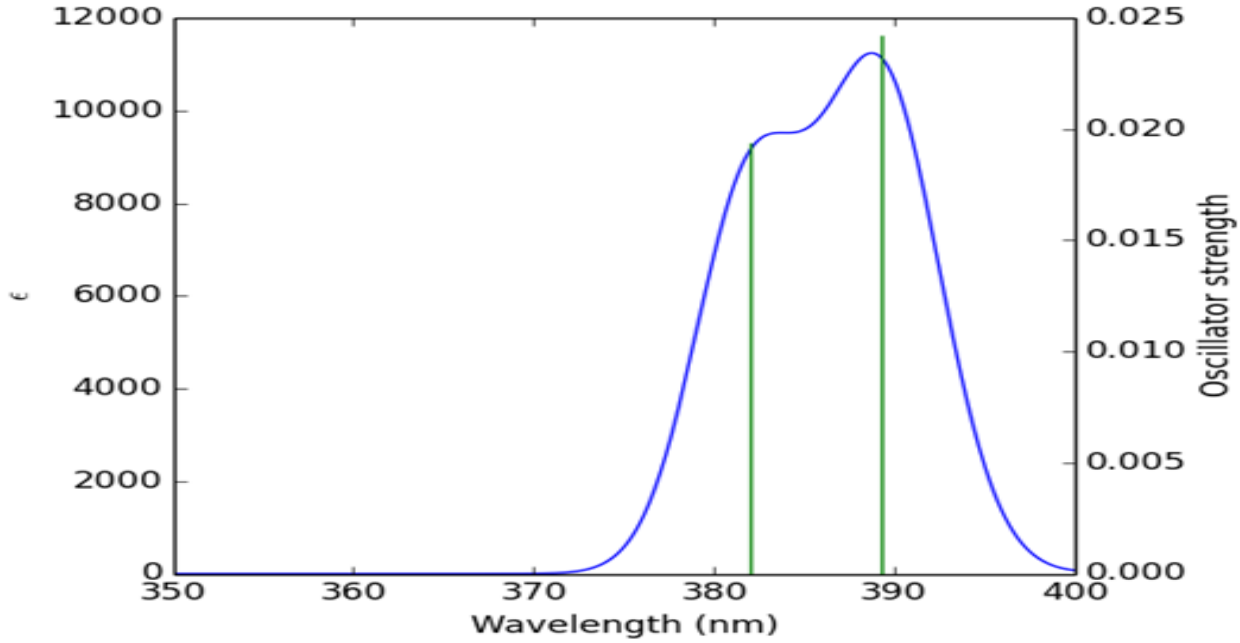

Fig. (3.18): UV-Vis spectrum for (PVA-SiC) (45 Atoms) using B3LYP/ LanL2DZ

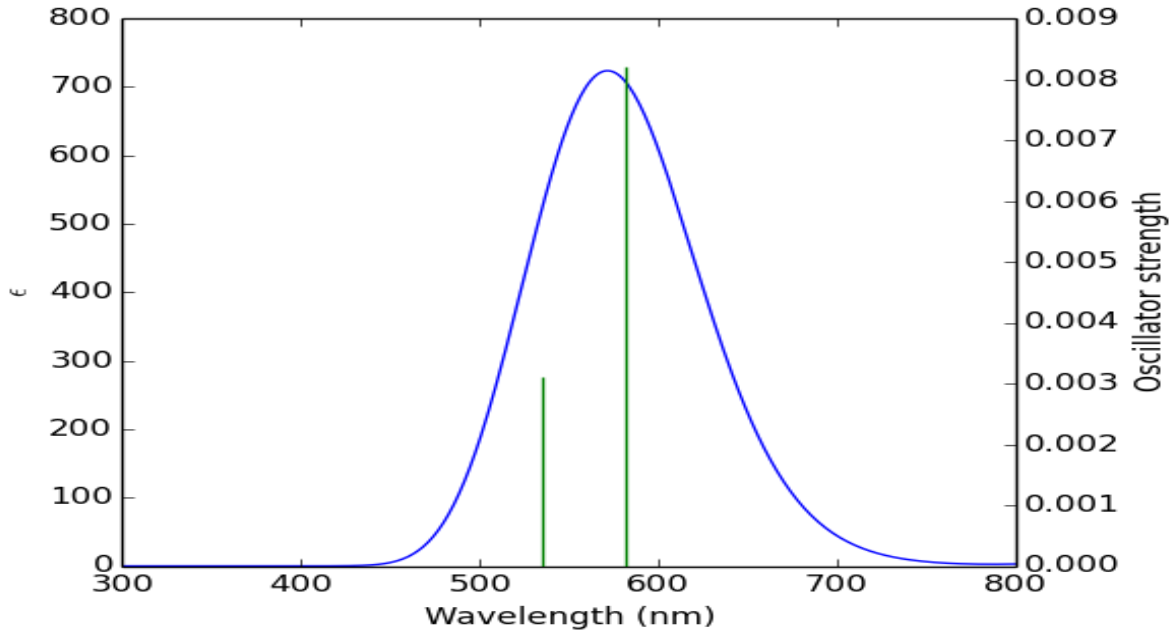

Fig. (3.19): UV-Vis spectrum for (PVA-SeO_2-SiC) (46 Atoms) using B3LYP/ LanL2DZ

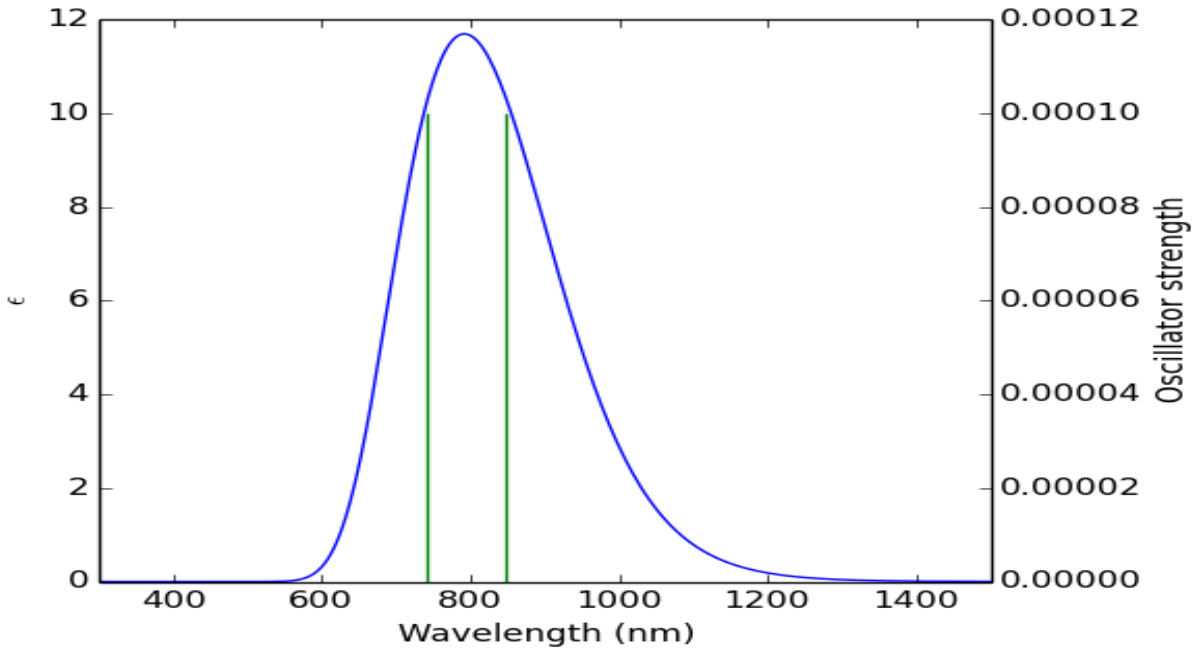

Fig. (3.20): UV-Vis spectrum for (PVA-SeO_2-SiC) (90 Atoms) using B3LYP/ LanL2DZ

3.4 Band Gap of (PVA-SeO_2-SiC) Nanocomposites

The band gap refers to energy difference between the highest occupied molecular orbital and lowest unoccupied molecular orbital according to Koopmans´ theorem. Table (3.2) shows the energy gap for nanocomposites (PVA) (43Atoms), (PVA-SiC) (45Atoms), (PVA-SeO_2-SiC) (46Atoms) and (PVA-SeO_2-SiC) (90Atoms) the results were close to the source [115,45]. Figures (3.21) - (3.24) show the 3-D distribution of HOMOs and LUMOs for the studied nanocomposites.

From these figures, the form of the nanocomposites has the same effect on both HOMO and LUMO distribution. The change in the form of the nanocomposites leads to a changing the map of HOMO and LUMO distribution according to the linear combination of atomic orbitals-molecular orbital LCAOs-MO.

The visualization of HOMO – LUMO obviously characterizes the electron cloud in occupied and virtual orbital.

Table (3.2): The values of energy gap in (eV) of the studied structures

PVA 43 Atoms			PVA-SiC 45 Atoms			PVA-SeO_2-SiC 46 Atoms			PVA-SeO_2-SiC 90 Atoms		
E_{HOMO} (eV)	E_{LUMO} (eV)	E_g (eV)	E_{HOMO} (eV)	E_{LUMO} (eV)	E_g (eV)	E_{HOMO} (eV)	E_{LUMO} (eV)	E_g (eV)	E_{HOMO} (eV)	E_{LUMO} (eV)	E_g (eV)
-5.933	0.922	6.856	-4.449	0.621	5.071	-5.931	-3.700	2.231	-6.057	-4.209	1.848

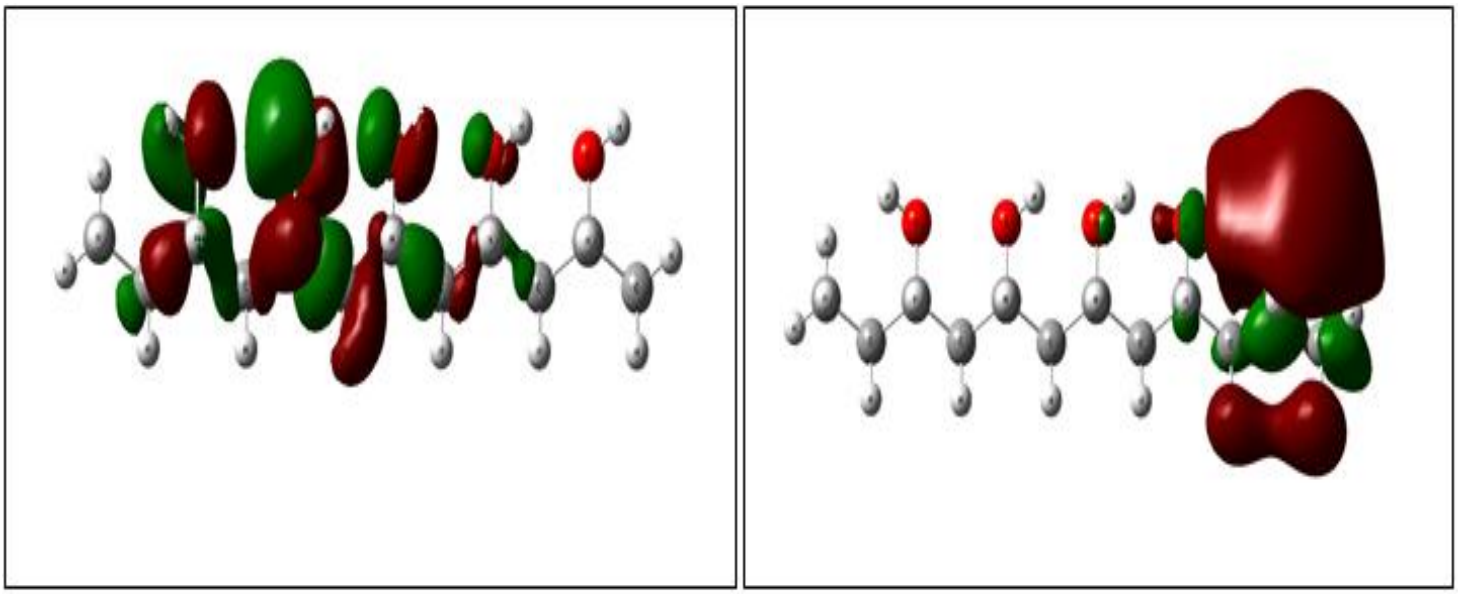

Fig. (3.21): The distribution of HOMO and LUMO for (PVA) (43 Atoms)

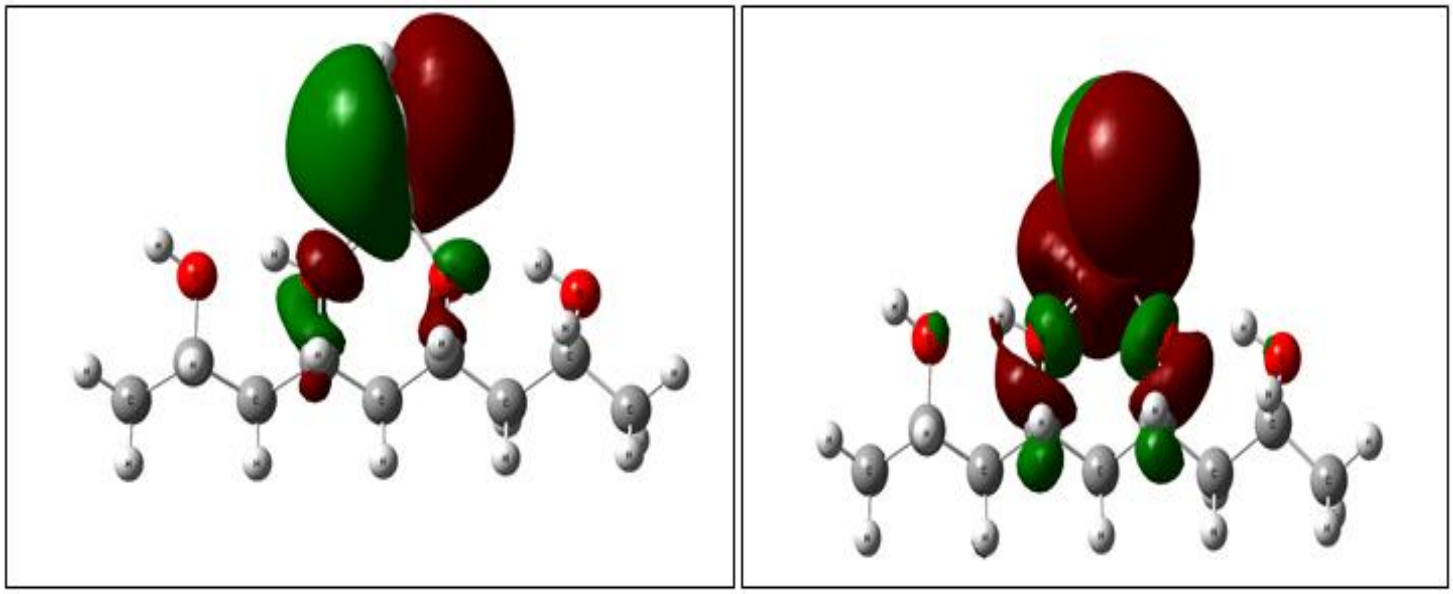

Fig. (3.22): The distribution of HOMO and LUMO for (PVA-SiC) (45 Atoms)

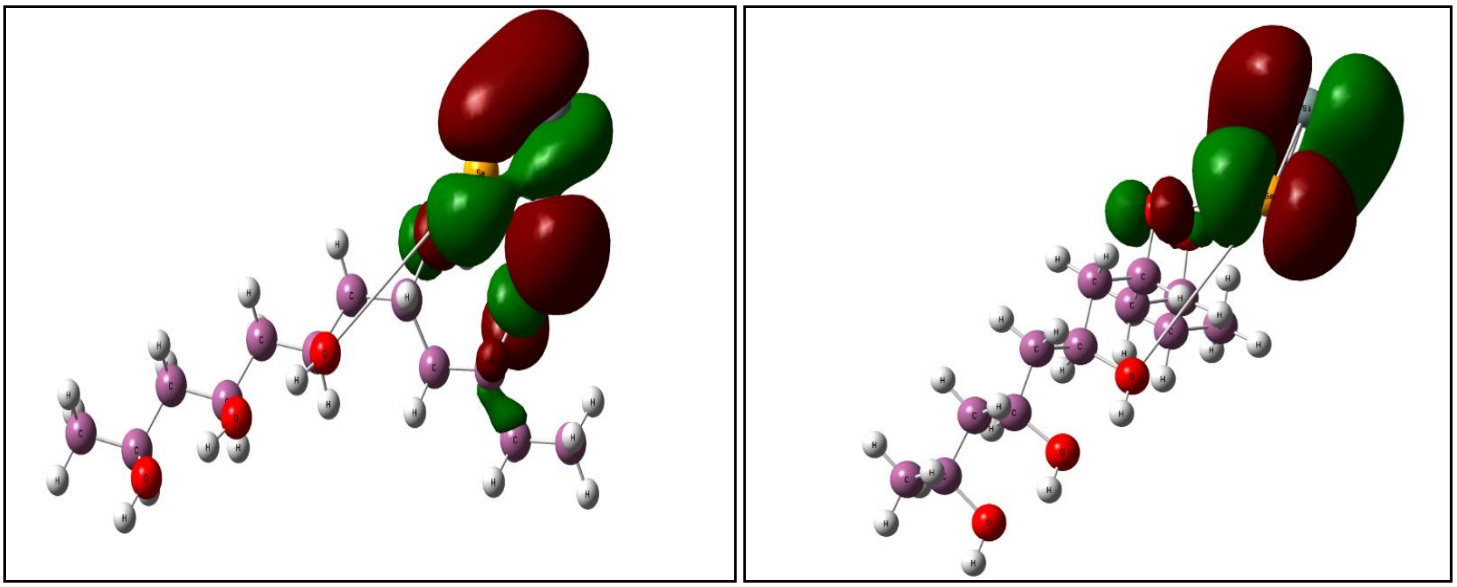

Fig. (3.23): The distribution of HOMO and LUMO for (PVA- SeO_2-SiC) (46 Atoms)

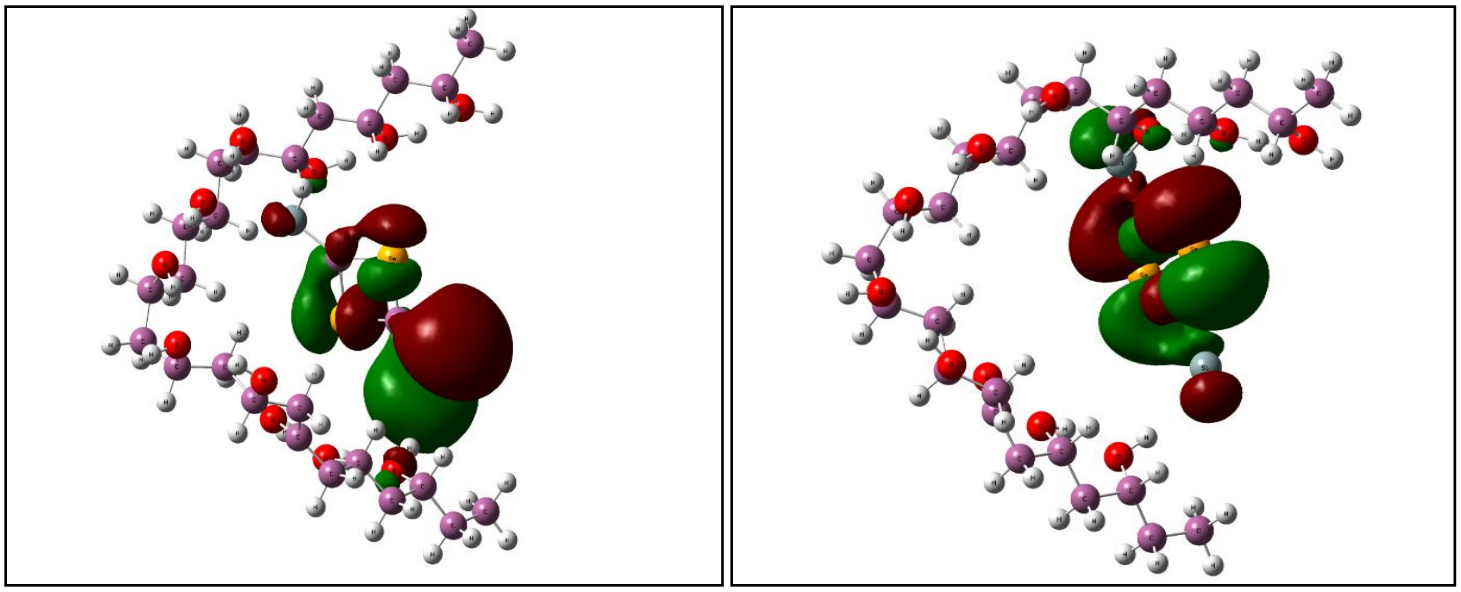

Fig. (3.24): The distribution of HOMO and LUMO for (PVA- SeO_2-SiC) (90 Atoms)

3.5 Electronic properties of (PVA-SeO_2-SiC) Nanocomposites

The computed total energy E_T and cohesive energy E_{coh} [relaxation energy, E_{rlx}, defined as the difference of the total energies of the nanocomposites and fully relaxed structures] [124,125] data shown in table (3.3) suggest that it decreases (in magnitude) with the increase in the number of atoms for all studied nanocomposites, this assign to that the total energy is a reflection of the binding energy. This indicates that the main contribution to the relaxation energy comes from the surface and sub-surface nanocomposites [45,124]. It is well known that the frontier molecular orbitals, HOMO and LUMO play a significant role for the reactant molecules in chemical reactions, it can be concluded that less negative E_{coh} value for nanocomposites might be related to its higher LUMO energy level. An interesting conclusion that can be drawn from these investigations is that this factor can affect the values of cohesive energies. Here, the system with larger E_{coh} is more stable. The hard molecule has a large energy gap and the soft molecule has a small energy gap. In quantum theory, changes in the electron density of system result from the mixing of suitable excited state wave functions with the ground state wave function. A small energy gap means small excitation energies to the manifold of excited states. Therefore, soft molecules with small energy gaps, their electron density change more easily than a hard molecule, and due to that, soft molecules will be more reactive than hard molecules [126].

The raising IP is the factor for the nanocomposites for electron acceptance and the large value of EA is the factor for determining the high ability to accepting an electron.

Low values of hardness η indicate easily electron transfer from valance to the conduction band, and this is a reflection to small band gap that the nanocomposites have.

The high values of chemical softness S means that the nanocomposites need small excitation energy for an electron transfer and a small energy gap it has. The values of electrophilicity in table (3.3) showed that the studied nanocomposites have great electrophilicity and this indicated to ability of the nanocomposites to accepting the electron more than donating. The nanocomposites which have high values of polarizability will be more effective, less stable, more softness and have small energy gap.

Table (3.3): The values of some electronic properties in eV of the studied structures

Property	PVA 43 Atoms	PVA-SiC 45 Atoms	PVA-SeO_2-SiC 46 Atoms	PVA-SeO_2-SiC 90 Atoms
Total energy	-23101.3339	-18984.9133	-24490.1177	-50980.76
cohesive energy	- 0.6885	-5.2744	-4.7739	-4.8911
Ionization potential	5.9339	4.4498	5.931	6.057
Electron affinity	0.9229	0.6217	3.700	4.209
Electronegativity	2.5055	1.9140	4.815	5.133
Chemical hardness	3.4284	2.5357	1.115	0.924
Chemical softness	0.1458	0.1971	0.448	0.541
Chemical potential	-2.5055	-1.9140	-4.815	-5.133
Electrophilicity	0.9155	0.7223	10.396	14.257
Dipole moment (Debye)	13.569	13.822	7.881	7.228
Polarizability (a.u)	144.647	148.601	224.586	458.586

3.6 Density of States

The strength of interactions can be further studied by analyzing orbital interactions between the atoms of the nanocomposite, in terms of density of states DOS as shown in Figures (3.25) - (3.28). The DOS governs many physical properties and consequently plays an important role in solid state physics, it is important to be able to predict how the DOS will behave for different molecular structures geometries. In all cases, the degeneracies of unoccupied molecular orbitals are more than the occupied molecular orbitals. The high density of states at specific energy levels refers to that there are many states in the structure available for occupation. If there are no states can be occupied at that energy level that refers to zero density of states. The measurements calculations indicate that the direction of electron transfer is from a transition metal to carbon and due to the increase in their electronegativity. The metal lattice expands and the metal–metal distance increases upon carbide formation, the increase in metal–metal distance causes contraction of the metal d-band and therefore would give a greater density of states (DOS) near the Fermi level [127].

The charge density is low in occupied orbital and high in virtual orbital for pure. This mentions the localization of charges along the virtual orbitals than in occupied orbitals.

The degenerate states as a function of energy levels for the studied structure, this degeneracy produced by the existence of the new types of atoms, and that leads to changing the bond lengths and angles or changing the geometry of the structure.

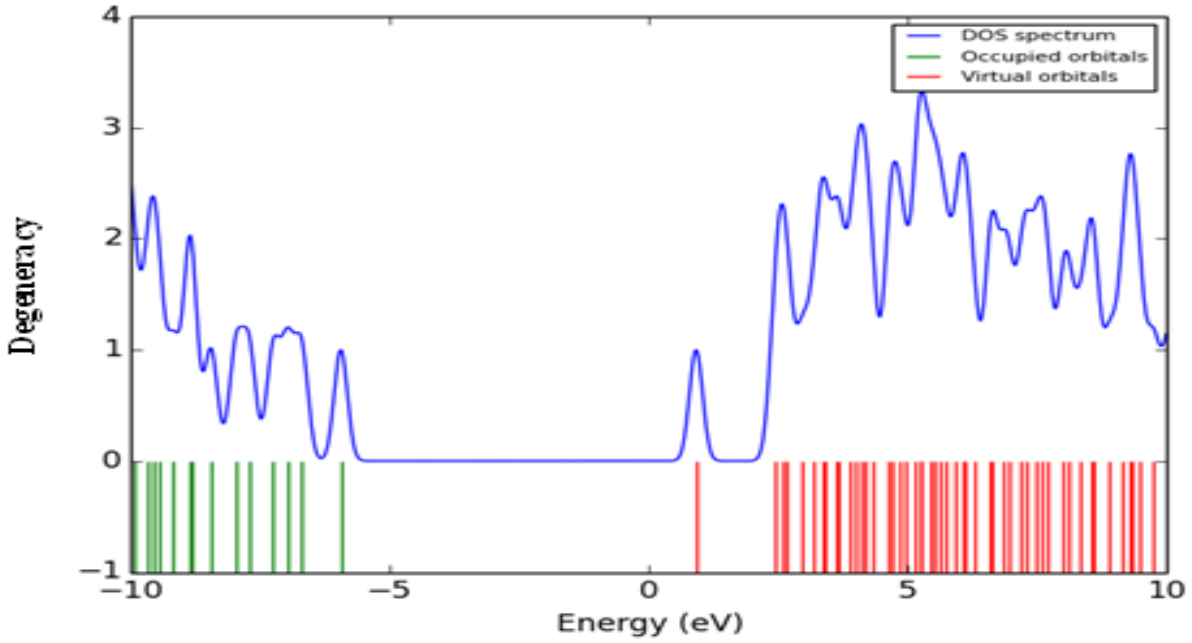

Fig. (3.25): The density of states as a function of bond length for (PVA) (43 Atoms)

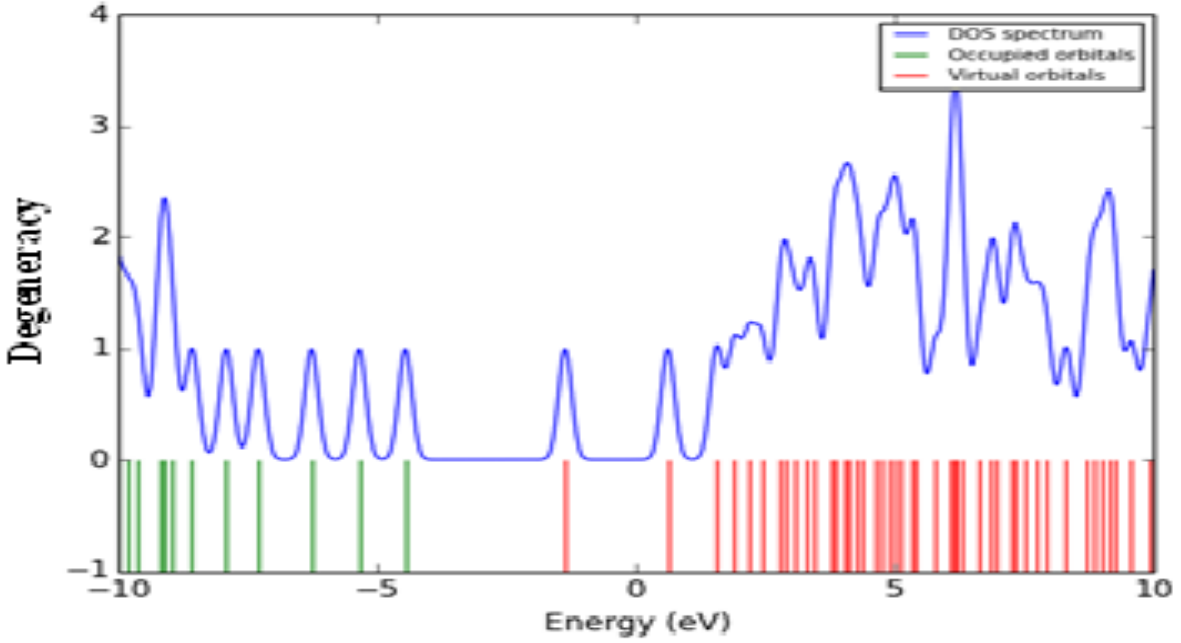

Fig. (3.26): The density of states as a function of bond length for (PVA-SiC) (45Atoms)

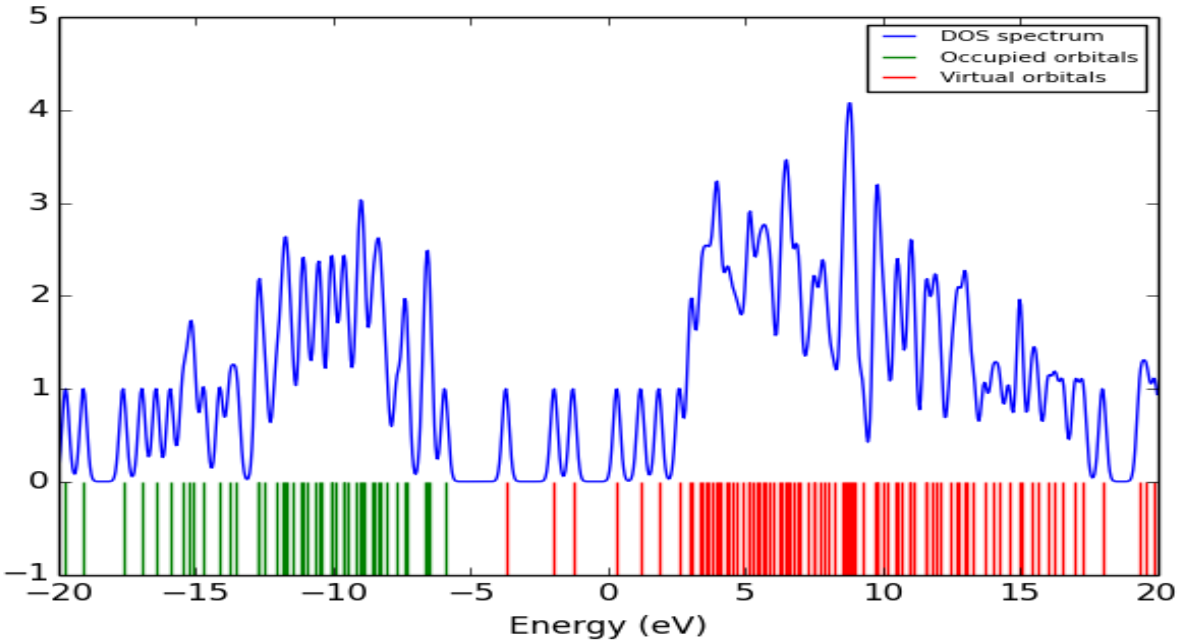

Fig. (3.27): The density of states as a function of bond length for (PVA-SeO_2-SiC) (46Atoms)

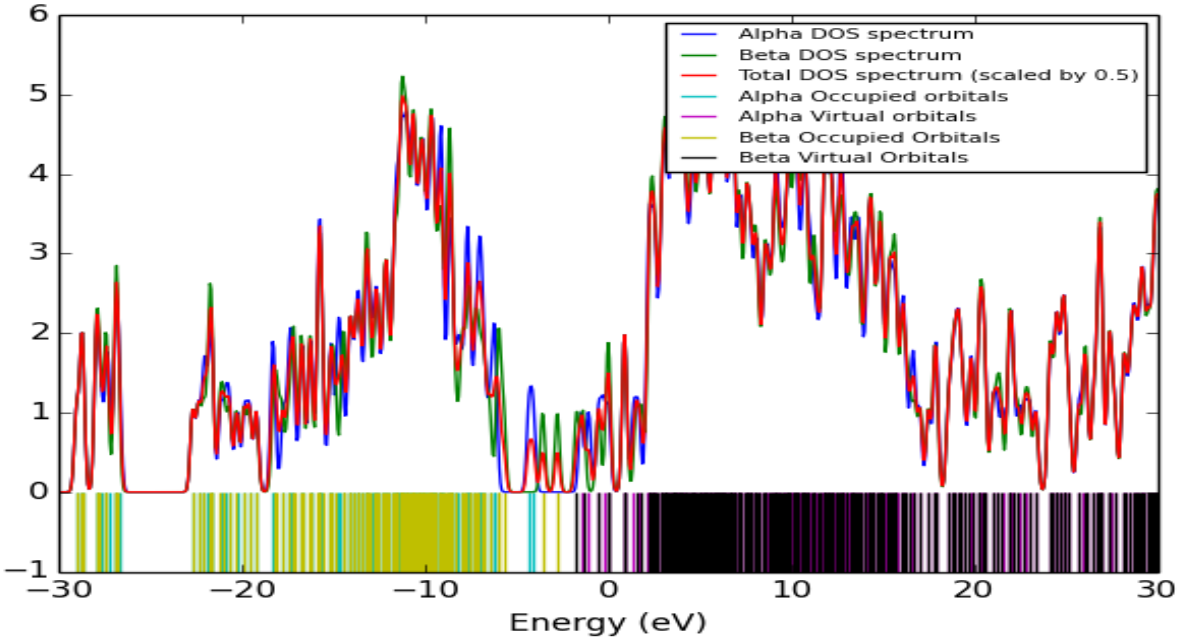

Fig. (3.28): The density of states as a function of bond length for (PVA-SeO_2-SiC) (90Atoms)

3.7 Electrostatic Potential of (PVA-SeO_2-SiC) Nanocomposites

Figures (3.29) - (3.32) show the electrostatic potential ESP distribution surface of nanocomposites calculated from the total self-consistent field SCF. The ESP distributions for the nanocomposites in result from the strength of repulsion or attraction of the areas that surround each nanocomposite. In general, the ESP surfaces of the (PVA) (43Atoms), (PVA-SiC) (45Atoms), (PVA-SeO_2-SiC) (46Atoms) and (PVA-SeO_2-SiC) (90Atoms) nanocomposites are dragged toward the positions of negative charges in each molecule means the oxygen atoms of high electronegativity.

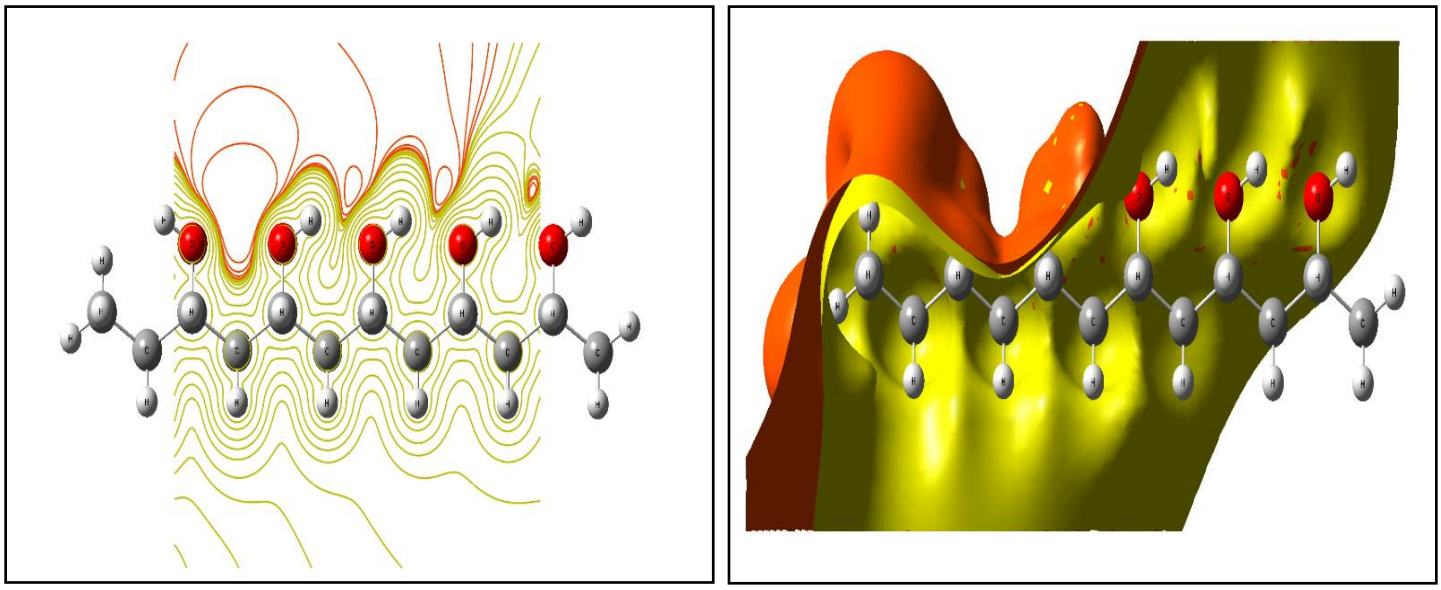

Fig. (3.29): The electrostatic potential distribution surface for (PVA) (43 Atoms) (left: 2-D counter; right: 3-D)

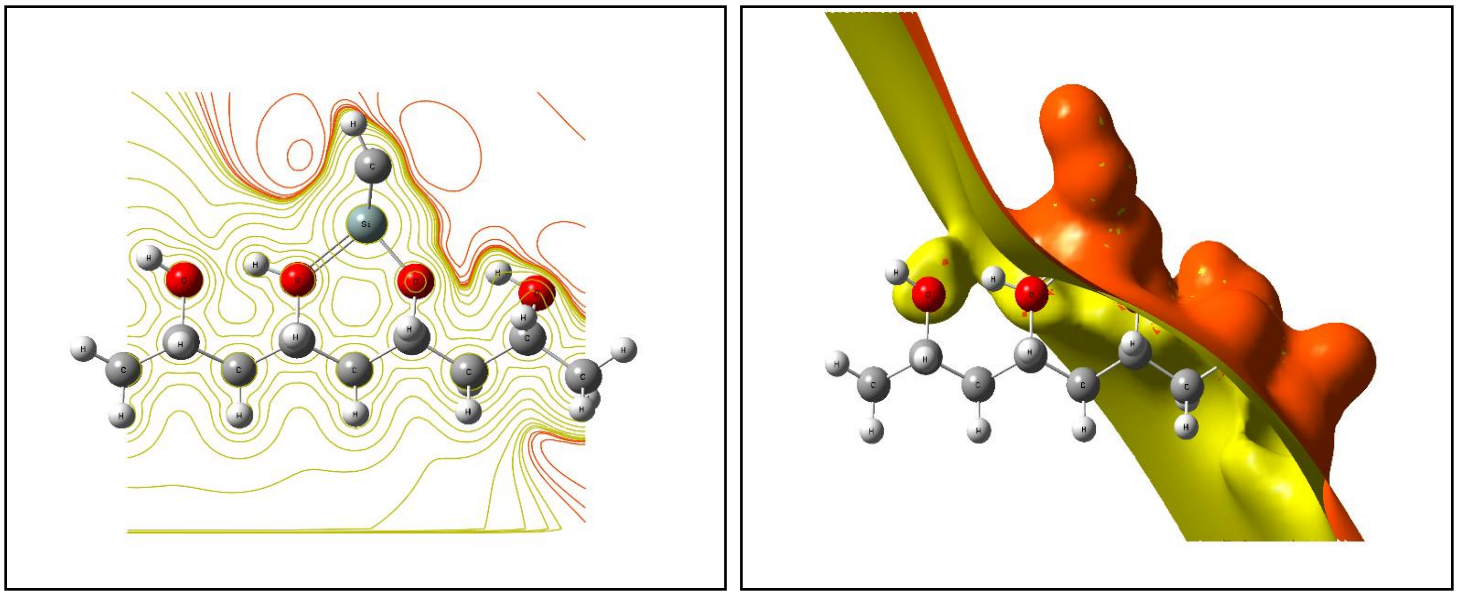

Fig. (3.30): The electrostatic potential distribution surface for (PVA-SiC) (45 Atoms) (left: 2-D counter; right: 3-D)

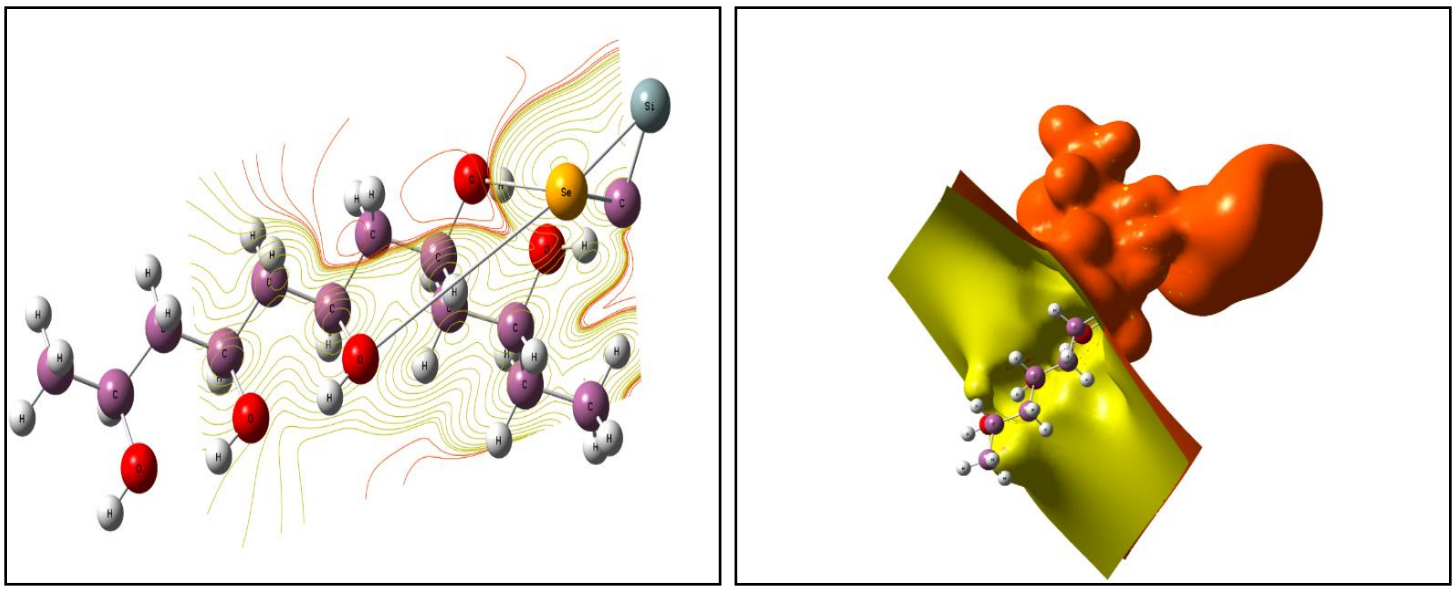

Fig. (3.31): The electrostatic potential distribution surface for (PVA-SeO_2-SiC)(46 Atoms) (left: 2-D counter; right: 3-D)

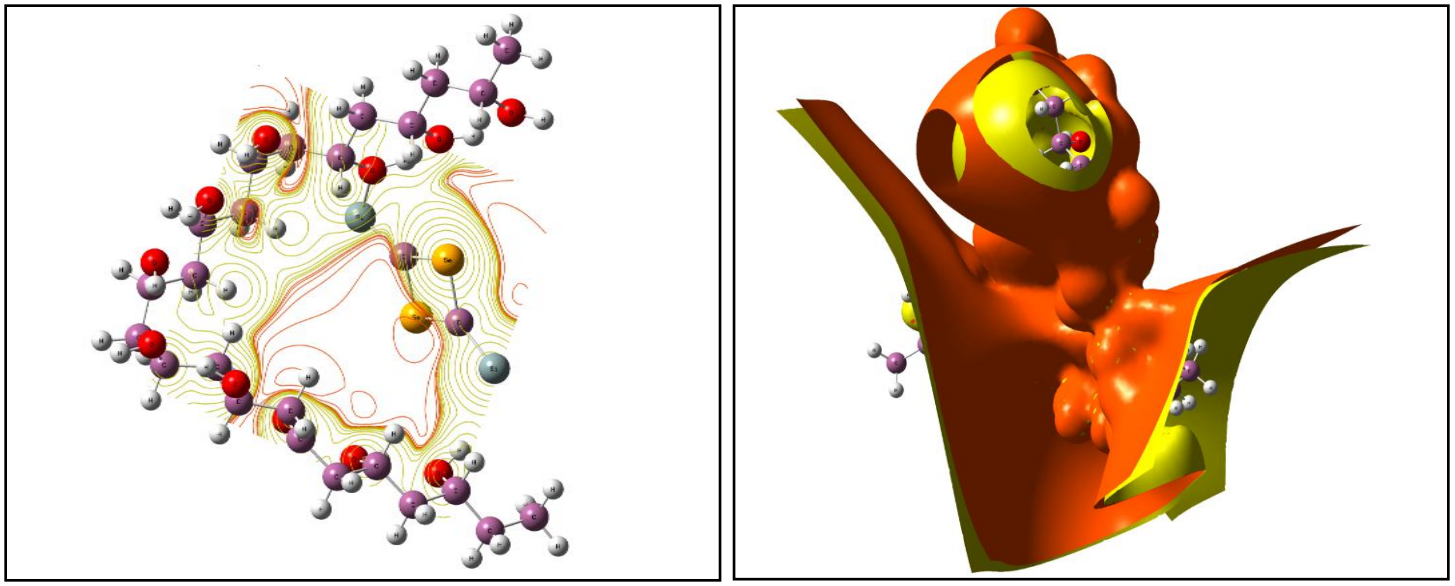

Fig. (3.32): The electrostatic potential distribution surface for (PVA-SeO_2-SiC)(90 Atoms) (left: 2-D counter; right: 3-D)

Chapter Four

Conclusions and Future Works

4.1 Conclusions

In this study, the hybrid functional B3LYP with LanL2DZ basis sets under the theoretical methodology density functional theory has been concerned.

1- The method (DFT) showed cogency in computing the geometric parameters of (PVA-SeO_2-SiC) nanocomposites because it's method is characterized by its accuracy to estimate the molecular properties of any compound. Good relax was obtained by B3LYP-DFT at Gaussian 0.9 package of the program and agree with that relax done by using the LanL2DZ.

2- The results showed decreasing of the energy gap from (6.856eV) to (1.848eV). This declares that these nanocomposites are the nearest to semiconductor because both HOMO and LUMO levels become more adjacent, which make it appropriate for many applications.

3- The IR studies show that adding nanoparticles leads to the displacement of some of the bonds and not the emergence of new peaks.

4- The stability increases when an increase in the number of atoms of nanoparticles, because decreasing the total energy and increases the cohesive energy.

5- With high resolution methods, which made it possible to separate ^1H NMR spectrum, interactions were characterized by ^1H NMR chemical shifts of SeO_2.

6- The results of UV-Vis spectra showed the spectrum in range (500-700 nm), which is within the limits of Visible light, so it has various applications such as optoelectronics such as LED.

7- The present calculations show that the cohesive energy (E_{coh}) increases with increasing the number of atoms of the nanocomposites.

8- All the studied nanocomposites need great energy to become an anion because ionization potential is increased with an increase in the number of atoms and the electronic affinity increase with an increase in the number of atoms.

9- The hardness decrease with an increase in the number of atoms, therefore all the nanocomposites are softer, and this reduces the resistance of a species to lose electrons.

10- The calculated values give a greater density of states (DOS) due to the increase in their electronegativity.

4.2 Suggestions for Future Works

Study on the following topics can be achieved:

1- Study of thermal properties of (PVA-SeO_2-SiC) nanocomposites.

2- Preparing experimentally studied nanocomposites and comparing practical results with theoretical results.

3- Study of the optical properties of (PVA-SeO_2-SiC) nanocomposites.

References

References

[1] Faraji, M., Yamini, Y., and Rezaee, M. (2010). Magnetic nanoparticles: synthesis, stabilization, functionalization, characterization, and applications. Journal of the Iranian Chemical Society, 7(1), 1-37.

[2] Chatterjee, S., SUBRAMANIAN, A., and SUBRAMANIAN, S. (2017). Synthesis and characterization of manganese dioxide using brassica oleracea (cabbage). Journal of Industrial Pollution Control, 33(2), 1627-1632.

[3] Snedden, E. (2011). Experimental investigations of excited-state dynamics in conjugated polymers using time-resolved laser spectroscopy (Doctoral dissertation, Durham University).

[4] Bower, D. I. (2003). An introduction to polymer physics.

[5] Zois, H., Apekis, L., and Omastová, M. (2001, June). Electrical properties of carbon black-filled polymer composites. In Macromolecular Symposia (Vol. 170, No. 1, pp. 249-256). Weinheim: WILEY-VCH Verlag GmbH.

[6] Knorowski, C. (2015). Dynamics and statics of polymer nanocomposite self-assembly via molecular dynamics (Doctoral dissertation, Iowa State University).

[7] Tsai, S. W., and Hahn, H. T. (1980). Introduction to composite materials (Vol.1).

[8] Jeon, I. Y., and Baek, J. B. (2010). Nanocomposites derived from polymers and inorganic nanoparticles. Materials, 3(6), 3654-3674.

[9] Hadi, S., Hashim, A., and Jewad, A. (2011). Optical properties of (PVA-LiF) composites. Australian Journal of Basic and Applied Sciences, 5(9), 2192-2195.

[10] Strumpler, R., and Glatz-Reichenbach, J. (1999). Conducting polymer composites. Journal of Electroceramics, 3(4), 329-346.

[11] Maldonado-Codina, C., and Efron, N. (2003). Hydrogel lenses-materials and manufacture. Optometry in Practice, 4, 101-113.

[12] Uzunpinar, C. (2010). Effect of dispersion of swcnts on the viscoelastic and final properties of epoxy based nanocomposites (Doctoral dissertation).

[13] Robertson, J. (2004). Realistic applications of CNTs. Materials Today, 7(10), 46-52.

[14] Delides, C. G. (2016). Everyday Life Applications of Polymer Nanocomposites. no. October.

[15] Lagashetty, A., and Venkataraman, A. (2005). Polymer nanocomposites. Resonance, 10(7), 49-57.

[16] Ariga, K., Hill, J. P., Lee, M. V., Vinu, A., Charvet, R., and Acharya, S. (2008). Challenges and breakthroughs in recent research on self-assembly. Science and technology of advanced materials.

[17] Nie, M., Sun, K., and Meng, D. D. (2009). Formation of metal nanoparticles by short-distance sputter deposition in a reactive ion etching chamber. Journal of applied physics, 106(5), 054314.

[18] Saxena, S. K. (2004). Polyvinyl alcohol (PVA). Chemical and Technical Assessment, 1(3), 3-5.

[19] Billmeyer, F. W. (1984). Textbook of polymer science. John Wiley and Sons.

[20] Rathod, S. G., Bhajantri, R. F., Ravindrachary, V., Sheela, T., Pujari, P. K., Naik, J., and Poojary, B. (2015). Pressure sensitive dielectric properties of TiO 2 doped PVA/CN-Li nanocomposite. Journal of Polymer Research, 22(2), 1-14.

[21] Mohammad Attaran, A., Hooshyari, K., Javanbakht, M., and Enhessari, M. Fabrication and Characterization of Poly Vinyl Alcohol/Poly Vinyl Pyrrolidone/MnTiO Nanocomposite Membranes for PEM Fuel Cells. Iranian (Iranica) Journal of Energy and Environment, 4(2).

[22] Sheha, E., Khoder, H., Shanap, T. S., El-Shaarawy, M. G., and El Mansy, M. K. (2012). Structure, dielectric and optical properties of p-type (PVA/CuI) nanocomposite polymer electrolyte for photovoltaic cells. Optik, 123(13), 1161-1166.

[23] Hassan, C. M., and Peppas, N. A. (2000). PVA Hydrogels, Anionic Polymerisation Nanocomposites. Biopolymers, 37-65.

[24] Mallakpour, S., and Barati, A. (2011). Efficient preparation of hybrid nanocomposite coatings based on poly (vinyl alcohol) and silane coupling agent modified TiO_2 nanoparticles. Progress in Organic Coatings, 71(4), 391-398.

[25] Finch, C. A. (Ed.). (1973). Polyvinyl alcohol; properties and applications. John Wiley and Sons.

[26] Gautam, A., and Ram, S. (2010). Preparation and thermomechanical properties of Ag-PVA nanocomposite films. Materials Chemistry and Physics, 119(1-2), 266-271.

[27] Baker, M. I., Walsh, S. P., Schwartz, Z., and Boyan, B. D. (2012). A review of polyvinyl alcohol and its uses in cartilage and orthopedic applications. Journal of Biomedical Materials Research Part B: Applied Biomaterials, 100(5), 1451-1457.

[28] Sharma, S. K., Prakash, J., Sudarshan, K., Sen, D., Mazumder, S., and Pujari, P. K. (2015). Structure at interphase of poly (vinyl alcohol)–SiC nanofiber composite and its impact on mechanical properties: positron annihilation and small-angle X-ray scattering studies. Macromolecules, 48(16), 5706-5713.

[29] Zhou, X. G., Wang, H. L., and Zhao, S. (2016). Progress of SiCf/SiC composites for nuclear application. Adv Ceram, 37, 151-167.

[30] Chaira, D., Mishra, B. K., and Sangal, S. (2006). Synthesis of silicon carbide by reaction milling in a dual-drive planetary mill. Society for Mining, Metallurgy, and Exploration, Inc..

[31] Chung, D. D. (2010). Composite materials: science and applications. Springer Science and Business Media.

[32] López-Antón, M. A., Díaz-Somoano, M., Fierro, J. L. G., and Martínez-Tarazona, M. R. (2007). Retention of arsenic and selenium compounds present in coal combustion and gasification flue gases using activated carbons. Fuel processing technology, 88(8), 799-805.

[33] Fan, Y., Zhuo, Y., and Li, L. (2017). SeO_2 adsorption on CaO surface: DFT and experimental study on the adsorption of multiple SeO_2 molecules. Applied Surface Science, 420, 465-471.

[34] Fan, Y., Zhuo, Y., Lou, Y., Zhu, Z., and Li, L. (2017). SeO_2 adsorption on CaO surface: DFT study on the adsorption of a single SeO_2 molecule. Applied Surface Science, 413, 366-371.

[35] Yan, R., Gauthier, D., Flamant, G., Peraudeau, G., Lu, J., and Zheng, C. (2001). Fate of selenium in coal combustion: volatilization and speciation in the flue gas. Environmental science and technology, 35(7), 1406-1410.

[36] Muñoz-Guillena, M. J., Linares-Solano, A., and de Lecea, C. S. M. (1994). A study of CaO-SO_2 interaction in the presence of O_2. Applied surface science, 81(4), 417-425.

[37] Li, Y. (2006). Experimental Study on Simultaneous Removal of Trace Selenium and Arsenic in Flue Gas Desulphurization within Medium Temperature Range. Tsinghua University: Beijing, China.

[38] Yang, G. Q., Wang, S. Z., Zhou, R. H., and Sun, S. Z. (1983). Endemic selenium intoxication of humans in China. The American journal of clinical nutrition, 37(5), 872-881.

[39] See, K. A., Lavercombe, P. S., Dillon, J., and Ginsberg, R. (2006). Accidental death from acute selenium poisoning. The Medical Journal of Australia, 185(7), 388-389.

[40] Agrawal, B. K., Yadav, P. S., and Yadav, R. K. (2012). Density Functional Theory Study of Small SiC Nanoclusters. Journal of Computational and Theoretical Nanoscience, 9(11), 1830-1849.

[41] Singh, R. S. (2016). Hydrogen adsorption on sulphur-doped SiC nanotubes. Materials Research Express, 3(7), 075014.

[42] Hosseinian, A., Khosroshahi, E. S., Nejati, K., Edjlali, E., and Vessally, E. (2017). A DFT study on graphene, SiC, BN, and AlN nanosheets as anodes in Na-ion batteries. Journal of molecular modeling, 23(12), 1-7.

[43] Peyravi, M., Arjmandi, M., Khakpour, R., and Jahanshahi, M. (2019). A chemisorption study of selenium dioxide on $C_{19}X$ (X= Ni, Cr and Cu) nanocage by DFT-based calculation. Surfaces and Interfaces, 16, 174-180.

[44] Hashim, A., Abduljalil, H., and Ahmed, H. (2019). Analysis of optical, electronic and spectroscopic properties of (biopolymer-SiC) nanocomposites for electronics applications. Egyptian Journal of Chemistry, 62(9), 1659-1672.

[45] Yaqoob, M., Gul, S., Zubair, N. F., Iqbal, J., and Iqbal, M. A. (2020). Theoretical calculation of selenium N-heterocyclic carbene compounds through DFT studies: Synthesis, characterization and biological potential. Journal of Molecular Structure, 1204, 127462.

[46] Ahmed, H., Hashim, A., and Abduljalil, H. M. (2020). Determination of optical parameters of films of PVA/TiO_2/SiC and PVA/MgO/SiC nanocomposites for optoelectronics and UV-detectors. Ukrainian Journal of Physics, 65(6), 533-533.

[47] Qu, W., Shen, F., Zu, H., Liu, S., Yang, J., Hu, Y., ... and Li, H. (2020). Density functional theory studies of the adsorption and interactions between

selenium species and mercury on activated carbon. Energy and Fuels, 34(8), 9779-9786.

[48] Ali, M., Islam, M. J., Rafid, M., Jeetu, R. R., Roy, R., and Chakma, U. (2021). The computational screening of structural, electronic, and optical properties for SiC, Si0. 94Sn0. 06C, and Si0. 88Sn0. 12C lead-free photovoltaic inverters using DFT functional of first principle approach. Eurasian Chemical Communications, 3(5), 327-38.

[49] Ahmed, H., and Hashim, A. (2021). Structural, optical and electronic properties of silicon carbide doped PVA/NiO for low cost electronics applications. Silicon, 13(5), 1509-1518.

[50] Andreoni, W., and Curioni, A. (2002). Towards the design of functional materials and drugs 'from Scratch'. Ercim News.

[51] Eschrig, H. (1996). The fundamentals of density functional theory (Vol. 32). Stuttgart: Teubner.

[52] Yong, D. C. (2001). Using existing basis sets. Computational Chemistry: A Practical Guide for Applying Techniques to Real-World Problems; John Wiley and Sons, Inc.: New York, NY, USA, 10, 78-98.

[53] Cox, P. A. (1996). Introduction to quantum theory and atomic structure. New York: Oxford University Press.

[54] Köhler, M., and Fritzsche, W. (2008). Nanotechnology: an introduction to nanostructuring techniques. John Wiley and Sons.

[55] Matthews, P. T. (1976). Introduction to quantum mechanics.

[56] Kaxiras, E. (2003). Atomic and electronic structure of solids (p. 696).

[57] Richardson, T. H. (Ed.). (2000). Functional organic and polymeric materials: molecular functionality-macroscopic reality. Wiley.

References

[58] Burroughs, J., Bradley, D., Brown, A., Marks, R. N., Mackey, K., Friend, R. H., ... and Holmes, A. B. (1990). Solid C60: a new form of carbon. Nature, 347, 539.

[59] Tang, C. L. (2005). Fundamentals of quantum mechanics: for solid state electronics and optics. Cambridge University Press.

[60] Manninen P. P. (2009) "Advanced Computational Chemistry" Lecture Notes for the Course.

[61] Valeev, E. F., and Sherrill, C. D. (2003). The diagonal Born–Oppenheimer correction beyond the Hartree–Fock approximation. The Journal of chemical physics, 118(9), 3921-3927.

[62] Sherrill, C. D. (2005). The born-oppenheimer approximation. School of Chemistry and Biochemistry, Georgia Institute of Technology, 242.

[63] Hollas, J. M. (2004). Modern spectroscopy. John Wiley and Sons.

[64] Rogers, D. W. (2003). Computational Chemistry using the PC. John Wiley and Sons.

[65] Fock, V. (1930). Näherungsmethode zur Lösung des quantenmechanischen Mehrkörperproblems. Zeitschrift für Physik, 61(1-2), 126-148.

[66] Valone, S. M. (2010). Quantal Density Functional Theory II. Approximation Methods and Applications.

[67] Fitts, D. D. (1999). Principles of quantum mechanics: as applied to chemistry and chemical physics. Cambridge University Press.

[68] Sholl, D., and Steckel, J. A. (2011). Density functional theory: a practical introduction. John Wiley and Sons.

[69] Bransden, B. H., and Joachain, C. J. (2003). Physics of atoms and molecules. Pearson Education India.

[70] Mueller, M. P. (2007). Fundamentals of quantum chemistry: molecular spectroscopy and modern electronic structure computations. Springer Science and Business Media.

[71] Kohanoff, J., and Gidopoulos, N. I. (2003). Density functional theory: basics, new trends and applications. Handbook of molecular physics and quantum chemistry, 2(Part 5), 532-568.

[72] Christopher, J. C. (2004). Essentials of computational chemistry: theories and models.

[73] Koch, W., and Holthausen, M. C. (2001). A Chemist's Guide to Density Functional Theory, Wiley.

[74] Parr, R. G., and Yang, W. (1994). Density-functional theory of atoms and molecules. International Series of Monographs on Chemistry. Oxford University Press, New York, 3, 14312-14321.

[75] Lipkowitz, K. B., Cundari, T. R., and Boyd, D. B. (Eds.). (2008). Reviews in computational chemistry (Vol. 51). John Wiley and Sons.

[76] Hutter, J. (2005). Lecture notes in computational chemistry electronic structure theory. Texto utilizado nos cursos no "Physical Chemistry Institute, University of Zurich.

[77] Jones, R. O. (2006). Introduction to density functional theory and exchange-correlation energy functionals. Computational Nanoscience: Do It Yourself, 31, 45-70.

[78] Kim, K., and Jordan, K. D. (1994). Comparison of density functional and MP2 calculations on the water monomer and dimer. The Journal of Physical Chemistry, 98(40), 10089-10094.

[79] Stephens, P. J., Devlin, F. J., Chabalowski, C. F., and Frisch, M. J. (1994). Ab initio calculation of vibrational absorption and circular dichroism spectra

using density functional force fields. The Journal of physical chemistry, 98(45), 11623-11627.

[80] Springborg, M. (2000). Methods of Electronic Structure Calculations, chapter 15.

[81] Camargo, A. J., Honório, K. M., Mercadante, R., Molfetta, F. A., Alves, C. N., and da Silva, A. B. (2003). A study of neolignan compounds with biological activity against Paracoccidioides brasiliensis by using quantum chemical and chemometric methods. Journal of the Brazilian Chemical Society, 14(5), 809-814.

[82] Udhayakala, P., and Rajendiran, T. V. (2011). Computational investigations on the corrosion inhibition efficiency of some pyridine based alkaloids. Journal of Chemical, Biological and Physical Sciences (JCBPS), 2(1), 172.

[83] Minkin, V. I. (1999). Glossary of terms used in theoretical organic chemistry. Pure and Applied Chemistry, 71(10), 1919-1981.

[84] Kampen, H. M., Méndez, H., and Zahn, D. R. T. (1999). Energy level alignment at molecular semiconductor/GaAs (100) interaces: Where is the LUMO. University of Chemnitz, Institut fur, Germany, 28.

[85] Dorsett, H., and White, A. (2000). Overview of molecular modelling and ab initio molecular orbital methods suitable for use with energetic materials. DEFENCE SCIENCE AND TECHNOLOGY ORGANIZATION SALISBURY (AUSTRALIA).

[86] Gotwals, R. R., and Sendlinger, S. C. (2007). A Chemistry Educator's Guide to Molecular Modeling. The North Carolina School of Science and Mathematics, Durham, NC.

[87] Reimers, J. R. (2011). Computational methods for large systems: electronic structure approaches for biotechnology and nanotechnology. John Wiley and Sons.

[88] Santos, J. C., Andres, J., Aizman, A., and Fuentealba, P. (2005). An aromaticity scale based on the topological analysis of the electron localization function including σ and π contributions. Journal of chemical theory and computation, 1(1), 83-86.

[89] Kwon, O., Coropceanu, V., Gruhn, N. E., Durivage, J. C., Laquindanum, J. G., Katz, H. E., ... and Brédas, J. L. (2004). Characterization of the molecular parameters determining charge transport in anthradithiophene. The Journal of chemical physics, 120(17), 8186-8194.

[90] Sherrill, C. D. (2002). Introduction to Electronic Structure Theory.

[91] Montalti, M., Credi, A., Prodi, L., and Gandolfi, M. T. (2006). Ionization energies, electron affinities, and reduction potentials. Handbook of Photochemistry, 3, 495-527.

[92] Bandyopadhyay, D. (2012). Chemisorptions effect of oxygen on the geometries, electronic and magnetic properties of small size Ni n (n= 1-6) clusters. Journal of molecular modeling, 18(2), 737-749.

[93] Weinert, M., Wimmer, E., and Freeman, A. J. (2008). Materials design application note. Phys. Rev, 26, 1-6.

[94] Fleming, I. (1976). Molecular orbitals and frontier orbitals. Frontier Orbitals and Organic Chemical Reactions (Fleming, I., Ed.), John Wiley and Sons, New York, 5-32.

[95] Abdulsattar, M. A. (2009). Size effects of semiempirical large unit cell method in comparison with nanoclusters properties of diamond - structured covalent semiconductors. Physica E: Low - dimensional Systems and Nanostructures, 41(9), 1679-1688.

[96] Hugosson, H. W. (2001). A theoretical treatise on the Electronic Structure of designer Hard Materials (Doctoral dissertation, Acta Universitatis Upsaliensis).

[97] Saito, T. (2004). "Inorganic Chemistry", Kanagawa University, D. I. Mendeleev publishes.

[98] Sabin, J. R., Trickey, S. B., Apell, S. P., and Oddershede, J. (2000). Molecular shape, capacitance, and chemical hardness. International Journal of Quantum Chemistry, 77(1), 358-366.

[99] Oftadeh, M., Naseh, S., and Hamadanian, M. (2011). Electronic properties and dipole polarizability of thiophene and thiophenol derivatives via density functional theory. Computational and Theoretical Chemistry, 966(1-3), 20-25.

[100] Sadasivam, K., and Kumaresan, R. (2011). Theoretical investigation on the antioxidant behavior of chrysoeriol and hispidulin flavonoid compounds–A DFT study. Computational and Theoretical Chemistry, 963(1), 227-235.

[101] Shenghua, L., He, Y., and Yuansheng, J. (2004). Lubrication chemistry viewed from DFT-based concepts and electronic structural principles. International Journal of Molecular Sciences, 5(1), 13-34.

[102] Barnes, C. E. (2003). Inorganic Chemistry (Catherine E. Housecroft and Alan G. Sharpe). Journal of Chemical Education, 80(7), 747.

[103] Judson, R. S., Jaeger, E. P., Treasurywala, A. M., and Peterson, M. L. (1993). Conformational searching methods for small molecules. II. Genetic algorithm approach. Journal of Computational Chemistry, 14(11), 1407-1414.

[104] Grant, W. B. (2002). An estimate of premature cancer mortality in the US due to inadequate doses of solar ultraviolet-B radiation. Cancer, 94(6), 1867-1875.

[105] Ketterer, B. (2011). Raman Spectroscopy of GaAs Nanowires: Doping Mechanisms and Fundamental Properties. École Polytechnique Fédérale de Lausanne.

[106] Ewing, G.W. and Woode, C. (1975). "Instrument Method of Analysis", McGraw-Hill.

[107] Abdulsattar, M. A., Hussein, M. T., and Hameed, H. A. (2014). Ab initio structural and vibrational properties of GaAs diamondoids and nanocrystals. AIP Advances, 4(12), 127119.

[108] John, C.D. and Kenneth, J.W. (2010). "Introduction to Physics" 8th edition, Wiley and Sons.

[109] Griffiths, P. R. (2002). Handbook of vibrational spectroscopy (Vol. 4). J. M. Chalmers (Ed.). Wiley.

[110] Pavia, D. L., Lampman, G. M., Kriz, G. S., and Vyvyan, J. A. (2008). Introduction to spectroscopy: cengage learning. Ainara López Maestresalas, 153, 752.

[111] Frisch, M., and Clemente, F. (2009). Gaussian 09, Revision A. 01, MJ Frisch, GW Trucks, HB Schlegel, GE Scuseria, MA Robb, JR Cheeseman, G. Scalmani, V. Barone, B. Mennucci, GA Petersson, H. Nakatsuji, M. Caricato, X. Li, HP Hratchian, AF Izmaylov, J. Bloino, G. Zhe.

[112] Parr, R. G., Donnelly, R. A., Levy, M., and Palke, W. E. (1978). Electronegativity: the density functional viewpoint. The Journal of Chemical Physics, 68(8), 3801-3807.

[113] Sarkar, J., Dey, P., Saha, S., and Acharya, K. (2011). Mycosynthesis of selenium nanoparticles. Micro and nano letters, 6(8), 599-602.

[114] Rybakov, V. B., Aslanov, L. A., Volkov, S. V., Grafov, A. V., Pekhn'o, V. I., and Fokina, Z. A. (1992). Crystal and molecular structures of the binuclear complex of rhodium (III) chloride with selenium dichloride and the complex

of iridium (III) chloride with sulfur dichloride and tetrachloride. Journal of Structural Chemistry, 33(3), 460-463.

[115] Wentz, K. E., Molino, A., Freeman, L. A., Dickie, D. A., Wilson, D. J., and Gilliard Jr, R. J. (2021). Reactions of 9 - Carbene - 9 - Borafluorene Monoanion and Selenium: Synthesis of Boryl - Substituted Selenides and Diselenides. Inorganic Chemistry, 60(18), 13941-13949.

[116] N. Arsalani, H. Fattahiand M. Nazarpoor. (2010). Synthesis and characterization of PVP-functionalized super paramagnetic Fe_3O_4 nanoparticles as an MRI contrast agent, 4, 329–338.

[117] D. Kumar, S.Karan Jat, P. K. Khanna, N. VijayanS. Banerjee. (2012). Synthesis, Characterization, and Studies of PVA/Co-Doped ZnO Nanocomposite Films, 4,408–416.

[118] Karthikeyan, K., Poornaprakash, N., Selvakumar, N., and Jeyasubrmanian, K. (2009). Thermal properties and morphology of MgO-PVA nanocomposite film. J Nanostruct Polym Nanocompos, 5(4), 83-88.

[119] Elmarzugi, N. A., Adali, T., Bentaleb, A. M., Keleb, E. I., Mohamed, A. T., and Hamza, A. M. (2014). Spectroscopic characterization of PEG-DNA biocomplexes by FTIR. Journal of Applied Pharmaceutical Science, 4(8), 6-10.

[120] Kumar, N. B., Crasta, V., and Praveen, B. M. (2014). Advancement in microstructural, optical, and mechanical properties of PVA (Mowiol 10-98) doped by ZnO nanoparticles. Physics Research International, Volume 2014, Article ID 742378, 9 pages.

[121] Larkin, P. (2017). Infrared and Raman spectroscopy: principles and spectral interpretation. Elsevier.

[122] Larkin, P. (2013). Infrared and Raman spectroscopy: principles and spectral interpretation, Elsevier Inc., ISBN 978-0-21-804162-8, 277 page.

[123] Incipini, L., Rongoni, E., Bagnoli, L., Marini, F., and Santi, C. (2012, October). New chiral electrophilic selenium reagents: synthesis and structural investigation. In Proceeding of the 16th International Electronic Conference on Synthetic Organic Chemistry, ECSOC-16.

[124] Bredow, T., Giordano, L., Cinquini, F., and Pacchioni, G. (2004). Electronic properties of rutile TiO_2 ultrathin films: Odd-even oscillations with the number of layers. Physical Review B, 70(3), 035419.

[125] Gerosa, M., Bottani, C. E., Caramella, L., Onida, G., Di Valentin, C., and Pacchioni, G. (2015). Electronic structure and phase stability of oxide semiconductors: Performance of dielectric - dependent hybrid functional DFT, benchmarked against G W band structure calculations and experiments. Physical Review B, 91(15), 155201.

[126] Ranade, M. R., Navrotsky, A., Zhang, H. Z., Banfield, J. F., Elder, S. H., Zaban, A., and Whitfield, H. J. (2002). Energetics of nanocrystalline TiO_2. Proceedings of the National Academy of Sciences, 99(2), 6476-6481.

[127] Oyama, S. T. (1992). Preparation and catalytic properties of transition metal carbides and nitrides. Catalysis today, 15(2), 179-200.

الخلاصة

تمت دراسة تأثير زيادة عدد الذرات على الخصائص الهندسية ، الالكترونية والطيفية للمتراكب النانوي ($PVA-SeO_2-SiC$) (بولي فينيل الكحول - ثنائي اوكسيد السيلينيوم - كاربيد السيليكون) وذلك باستخدام برنامج Gaussian 0.9 وبمساعدة Gaussian View 0.5 .

تم اجراء جميع الحسابات باستخدام نظرية دالية الكثافة (Density Functional Theory) (DFT) ، ويتم وصف تفاعل التبادل - الارتباط بواسطة الدالة الهجينة (B3LYP) (Becks 3-parameter Lee - Yang - Parr -) مع تقريب التدرج العام (General Gradient Approximation) (GGA) مع مجموعة الأساس (LanL2DZ).

دُرست الخصائص الهندسية ، الالكترونية و الطيفية لبوليمر (بولي فينيل الكحول) (PVA) (43Atoms) ومن ثم دراسة تأثير اضافة جسيمات نانوية كاربيد السيليكون (SiC) الى البوليمر (PVA) ليصبح المتراكب النانوي (PVA-SiC) (45Atoms) وبعدها تم اضافة جسيمات نانوية (SeO_2) بمرحلتين ($PVA-SeO_2-SiC$) (46Atoms) و ($PVA-SeO_2-SiC$) (90Atoms) .

تضمنت الخصائص الهندسية تحسين الأمثلية الهندسية (الاواصر والزوايا) . وشملت الخصائص الالكترونية (الجهد الايوني ، التقارب الالكتروني ، الصلادة الكيميائية ، الليونة الكيميائية ، الكهروسلبية ، الطاقة الكلية ، معدل طاقة الربط ، فجوة الطاقة ، الالفة الالكترونية وكثافة الحالات) ، وكذلك الخصائص الطيفية والتي تضمنت (الأشعة تحت الحمراء ، طيف رامان ، الأشعة فوق البنفسجية - المرئية و الرنين النووي المغناطيسي). اظهرت النتائج أن زيادة عدد ذرات المتراكبات النانوية له تأثير مباشر على جميع خصائص الهيكل المدروس.

ان اضافة الجسيمات النانوية وزيادة عدد ذراتها تباعاً ادى الى تحسين كبير في الخصائص المدروسة ومنها فجوة الطاقة التي تناقصت من (6.856eV) لبوليمر (PVA) الى (1.848eV) للمتراكب النانوي ($PVA-SeO_2-SiC$) (90Atoms) . كما لوحظ تحسن كبير في الخصائص الالكترونية ، حيث اظهرت النتائج أن طاقة الترابط ، جهد التأين ، الكهروسلبية ، الالفة الالكترونية ، الليونة الكيميائية ، والاستقطاب للمتراكب ($PVA-SeO_2-SiC$) قد ازدادت ، بينما الصلادة الكيميائية تتناقص . لقد تم أيجاد أشكال مختلفة للجهد الكهروستاتيكي وكثافة الحالات في كل تركيب. بشكل عام، إن النتائج التي تم التوصل اليها في هذه الدراسة تشير الى بناء تراكيب جديدة لها خواص الكترونية جديدة مختلفة.

جمهورية العراق
وزارة التعليم العالي والبحث العلمي
جامعة بابل ـ كلية التربية للعلوم الصرفة
قسم الفيزياء

تأثير كاربيد السليكون على الخصائص الالكترونية والطيفية لهيكل PVA/SeO_2 . دراسة دالية الكثافة الوظيفية

رسالة مقدمة

إلى مجلس كلية التربية للعلوم الصرفة في جامعة بابل وهي جزء من متطلبات

نيل درجة الماجستير في التربية / الفيزياء

من قبل

صفا زهير حسين عباس

بكالوريوس تربية علوم (فيزياء)

جامعة بابل 2010 م

بأشراف

أ.م.د. هند احمد محمد رؤوف ياسين

1444هـ **2022 م**